CHIMERIC FLORAL ORGANS1, Encoding a Monocot-Specific MADS Box Protein, Regulates Floral Organ Identity in Rice[1][C][W]

Xianchun Sang[2], Yunfeng Li[2], Zengke Luo[2], Deyong Ren, Likui Fang, Nan Wang, Fangming Zhao, Yinghua Ling, Zhenglin Yang, Yongsheng Liu, and Guanghua He*

Rice Research Institute (X.S., Y.Li, Z.L., D.R., L.F., N.W., F.Z., Y.Ling, Z.Y., G.H.), Chongqing Key Laboratory of Application and Safety Control of Genetically Modified Crops (X.S., Y.Li, D.R., L.F., F.Z., Z.Y., G.H.), and Engineering Research Center of South Upland Agriculture, Ministry of Education (Z.L., Y.Ling, G.H.), Southwest University, Chongqing 400715, China; and School of Biotechnology and Food Engineering, Hefei University of Technology, Hefei 230009, China (Y.Liu)

The control of floral organ identity by homeotic MADS box genes is well established in eudicots. However, grasses have highly specialized outer floral organs, and the identities of the genes that regulate the highly specialized outer floral organs of grasses remain unclear. In this study, we characterized a MIKC-type MADS box gene, *CHIMERIC FLORAL ORGANS* (*CFO1*), which plays a key role in the regulation of floral organ identity in rice (*Oryza sativa*). The *cfo1* mutant displayed defective marginal regions of the palea, chimeric floral organs, and ectopic floral organs. Map-based cloning demonstrated that *CFO1* encoded the OsMADS32 protein. Phylogenetic analysis revealed that *CFO1*/*OsMADS32* belonged to a monocot-specific clade in the MIKC-type MADS box gene family. The expression domains of *CFO1* were mainly restricted to the marginal region of the palea and inner floral organs. The floral organ identity gene *DROOPING LEAF* (*DL*) was expressed ectopically in all defective organs of *cfo1* flowers. Double mutant analysis revealed that loss of *DL* function mitigated some of the defects of floral organs in *cfo1* flowers. We propose that the *CFO1* gene plays a pivotal role in maintaining floral organ identity through negative regulation of *DL* expression.

Most flowers consist of four distinct organ types arranged in concentric whorls: sepals (whorl 1), petals (whorl 2), stamens (whorl 3), and carpels and ovules (whorl 4). The well-established ABCDE model, which is mainly based on genetic and molecular studies involving eudicots, such as Arabidopsis (*Arabidopsis thaliana*), snapdragon (*Antirrhinum majus*), and petunia (*Petunia hybrida*), explains how floral organ identity is coordinately defined by A-, B-, C-, D-, and E-class MADS box genes in eudicots (Coen and Meyerowitz, 1991; Weigel and Meyerowitz, 1994; Theissen and Saedler, 2001; Ditta et al., 2004).

The Poaceae, one of the largest monocot families, includes many important crops, such as barley (*Hordeum vulgare*), maize (*Zea mays*), rice (*Oryza sativa*), and wheat (*Triticum aestivum*). The floral architecture of grass species is distinct from those of eudicots and other monocots. The spikelet, the basic unit of the grass inflorescence, consists of glumes and one to 40 florets that comprise the lemma and palea (possibly homologous to sepals), lodicules (homologous to petals), stamens, pistils, and ovules (Bommert et al., 2005; Itoh et al., 2005; Malcomber et al., 2006). The recent characterization of several MADS box genes that specify floral organ identity in rice suggests that the ABCDE model applies to the regulation of stamen, pistil, and ovule development in grass species, at least in part (Nagasawa et al., 2003; Yamaguchi et al., 2006; Dreni et al., 2007; Yao et al., 2008). However, the molecular mechanisms that control the specification of grass-specific floral organs (the lemma, palea, and lodicule) remain to be elucidated.

The B-class genes are well conserved between Arabidopsis and rice. The Arabidopsis B-class genes *APETALA3* (*AP3*) and *PISTILLATA* (*PI*) are required to specify petal and stamen identities (Bowman et al., 1989; Goto and Meyerowitz, 1994; Jack et al., 1994). The *OsMADS16*/*SUPERWOMAN1* (*SPW1*) and *OsMADS4*

[1] This work was supported by the 863 Program of China (grant nos. 2006AA10Z167 and 2011AA10A100), the National Natural Science Foundation of China (grant nos. 30700451 and 31271304), the Fundamental Research Funds for the Central Universities (XDJK2012A001), the Excellent Youth Foundation of the Chongqing Scientific Committee (grant no. 2008BA1033), and the Chongqing Major Scientific and Technological Research Project (grant no. 2010AA1013).

[2] These authors contributed equally to the article.

* Corresponding author; e-mail hegh1968@yahoo.com.cn.

The author responsible for distribution of materials integral to the findings presented in this article in accordance with the policy described in the Instructions for Authors (www.plantphysiol.org) is: Guanghua He (hegh1968@yahoo.com.cn).

[C] Some figures in this article are displayed in color online but in black and white in the print edition.

[W] The online version of this article contains Web-only data.

www.plantphysiol.org/cgi/doi/10.1104/pp.112.200980

genes, the orthologs of Arabidopsis *AP3* and *PI*, determine the lodicule and stamen identities in rice (Nagasawa et al., 2003; Xiao et al., 2003; Yao et al., 2008). The *OsMADS2* gene, a paralog of *OsMADS4* in rice, mainly functions in lodicule specification (Prasad and Vijayraghavan, 2003; Yadav et al., 2007; Yao et al., 2008).

The C-class gene *AGAMOUS* (*AG*) is a key regulator of stamen and carpel identities and floral meristem determinacy in Arabidopsis (Bowman et al., 1991; Drews et al., 1991). Two C-class paralogs, *OsMADS3* and *OsMADS58*, which are orthologous to *AG*, play distinct roles in developmental regulation of the lodicule, stamen, and pistil in rice (Yamaguchi et al., 2006). More intriguingly, *DROOPING LEAF* (*DL*), an ortholog of the Arabidopsis *YABBY* gene *CRABS CLAW* (*CRC*), plays pivotal roles in pistil specification and floral meristem determinacy and antagonizes the function of B-class genes in rice (Bowman and Smyth, 1999; Yamaguchi et al., 2004). In Arabidopsis, the D-class gene *SEEDSTICK* (*STK*) acts redundantly with the C-class genes *AG* and *SHATTERPROOF1/2* to determine ovule identity (Pinyopich et al., 2003). In rice, two *STK*-like genes have been identified: whereas *OsMADS13* is required for ovule specification, the function of *OsMADS21* remains unclear (Dreni et al., 2007).

In Arabidopsis, the A-class genes *AP1* and *AP2* specify sepal and petal identities (Mandel et al., 1992; Jofuku et al., 1994). The E-class genes *SEPALLATA1/2/3/4* (*SEP1/2/3/4*) redundantly specify all floral organ identities and floral meristem determination (Pelaz et al., 2000; Ditta et al., 2004). In rice, three *AP1*-like genes and five *SEP*-like genes are known, of which only three have been characterized (Fornara et al., 2003; Malcomber and Kellogg, 2004, 2005; Kater et al., 2006). The *SEP*-like gene *OsMADS1/LEAFY HULL STERILE* (*LHS1*) is required for the specification of lemma and palea identity (Jeon et al., 2000; Agrawal et al., 2005; Prasad et al., 2005; Chen et al., 2006). Recently, another *SEP*-like gene, *OsMADS34/PANICLE PHYTOMER2*, was found to control rudimentary glume and sterile lemma development (Kobayashi et al., 2010). An *AP1/FRUITFULL*-like gene, *OsMADS15/DEGENERATIVE PALEA* (*DEP*), specifies palea and sterile lemma identity (Wang et al., 2010).

All of the above ABCDE floral regulators, except Arabidopsis *AP2*, belong to several classes of MIKC-type MADS box genes. The role of a special class of MIKC-type MADS box genes, which includes rice *OsMADS32* and its orthologs, still remains to be elucidated (Ma et al., 1991; Nam et al., 2004; Arora et al., 2007). In this study, we characterized a spontaneous mutant named *chimeric floral organs1* (*cfo1*). Molecular cloning indicated that the underlying allele of *CFO1* encoded the OsMADS32 protein. Phenotypic analysis revealed that the loss of function of *CFO1* led to defective marginal regions of the palea, chimeric floral organs, and ectopic organs. *CFO1* expression was detected throughout the meristematic region of the inflorescence and flower before initiation of the floral organs. Subsequently, the expression domains became mainly restricted to the marginal regions of the palea and inner floral organs. Expression and double mutant analysis suggested that CFO1 repressed *DL* transcription. We conclude that *CFO1* plays a pivotal role in maintaining floral organ identity by negative regulation of *DL* expression.

RESULTS

Alteration of Floral Organ Identity in *cfo1*

The developmental stages of rice described by Ikeda et al. (2004) were applied in this study. The morphology of *cfo1* and wild-type flowers was compared at the inflorescence 9 stage (heading stage). A typical wild-type rice flower is composed of a pistil in the central whorl (whorl 4), six stamens around the pistil in whorl 3, two lodicules adjacent to the lemma in whorl 2, and two interlocking organs (the palea and lemma, collectively termed the hull) that surround the inner floral organs in whorl 1 (Figs. 1, A, C, and I, and 2, A-1 and A-5).

In *cfo1* flowers, the most obvious alterations were split florets and bent paleas with broad marginal regions. Loss of the hook from the palea disrupted the mechanism by which this structure normally interlocks with the counterpart hook of the lemma (Fig. 1, B and H; Supplemental Fig. S1A). Further examination showed that the identity of the marginal region of the palea (mrp) of *cfo1* flowers was not well established. The wild-type palea consists of two parts: the body of the palea (bop) and two mrp (Ohmori et al., 2009; Fig. 1, C, E, and G). The bop, which has a texture similar to that of the lemma, was composed of a silicified upper epidermis that bore trichomes and protrusions, fibrous sclerenchyma, spongy parenchyma, and a vacuolated inner epidermis (Fig. 1I; Prasad et al., 2005). The mrp had a distinct cellular structure that contained a nonsilicified upper epidermis without trichomes and protrusions (Fig. 1E), a large number of spongy parenchyma cells, a few fibrous sclerenchyma cells, and a nonvacuolated inner epidermis (Fig. 1I; Prasad et al., 2005). However, in *cfo1* flowers, the mrp was converted to a lemma-like structure with silicified upper epidermal cells (Fig. 1F) and vacuolated inner epidermal cells (Fig. 1J). In addition, the *cfo1* palea was significantly wider than that of the wild type because of its expanded mrp, which was similar in width to that of the lemma (Supplemental Fig. S1B).

Expression of the ABCDE-class genes and the *CRC*-like gene *DL* was evaluated in the lemmas and paleas of wild-type and *cfo1* flowers with quantitative reverse transcription (qRT)-PCR. In wild-type flowers, *DL* was expressed in the lemma but not in the palea (Yamaguchi et al., 2004; Supplemental Fig. S2A). However, in *cfo1* flowers, significant expression of *DL* was detected in the palea (Supplemental Fig. S2A), which suggested that the *cfo1* palea acquired some degree of lemma

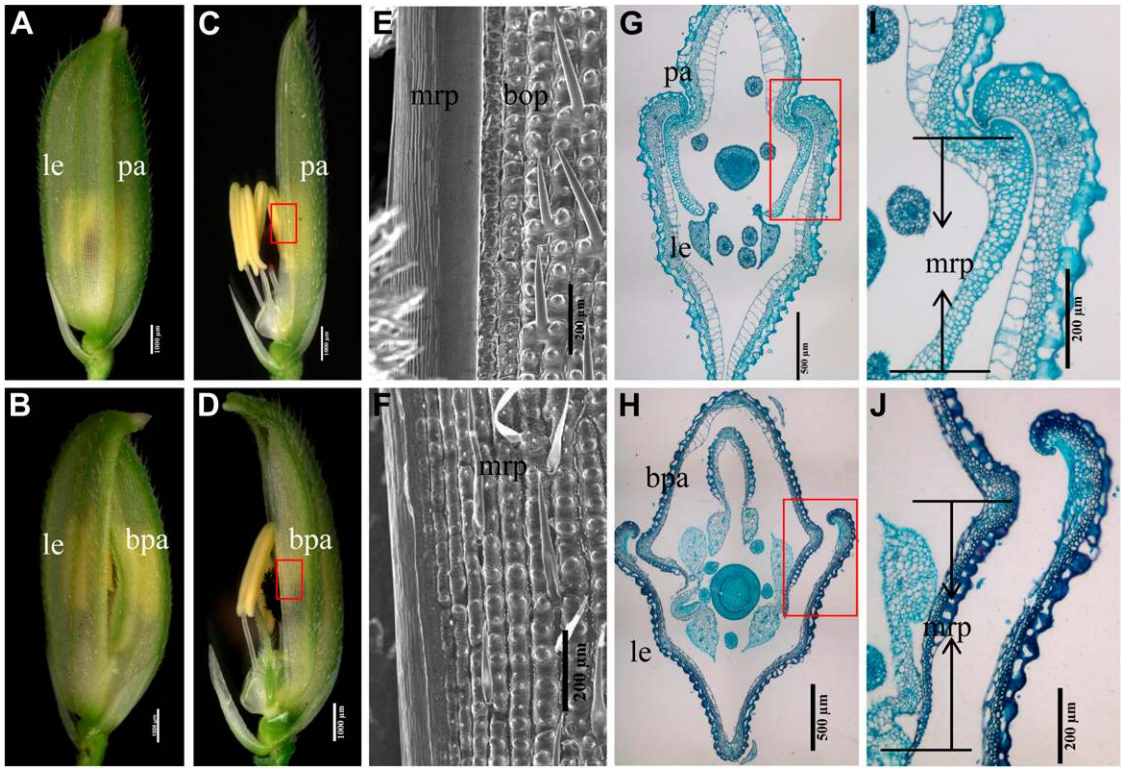

Figure 1. Palea identity in *cfo1* and wild-type flowers. A and B, Spikelets of wild-type (A) and *cfo1* (B) flowers. C and D, Spikelets of wild-type (C) and *cfo1* (D) flowers. The lemmas have been removed. The mrp in *cfo1* flowers is larger than that in wild-type flowers. E and F, Scanning electron micrographs of the mrp in wild-type (E) and *cfo1* (F) flowers. G and H, Transverse sections of wild-type (G) and *cfo1* (H) spikelets. I and J, Transverse sections through the margin between the lemma and palea in wild-type (I) and *cfo1* (J) flowers. bpa, Bent palea; le, lemma; pa, palea. Bars = 1,000 μm in A to D, 500 μm in G and H, and 200 μm in E, F, I, and J. [See online article for color version of this figure.]

identity. The expression of the other genes was similar in the paleas of wild-type and *cfo1* flowers.

The lemma and palea were removed for analysis of the phenotypes of the inner floral organs. Severely defective morphogenesis of the inner floral organs was observed in *cfo1* flowers.

In whorl 2, the wild-type lodicule was a small, fleshy, cup-shaped, nonphotosynthetic organ (Fig. 2A-1) with smooth epidermal cells (Fig. 2A-2). The lodicule contained parenchymatous cells interspersed with tracheal elements (Fig. 2A-5; Yadav et al., 2007). However, elongated lodicules that carried hull- and/or pistil-like tissues were observed in the majority of *cfo1* flowers (Fig. 2, B and C; Supplemental Fig. S1A). Figure 2B shows the hull-lodicule chimeras in *cfo1* flowers. Lodicule-like tissues were observed in the marginal regions of the base, whereas hull-like tissues developed along the medial axis (Fig. 2, B-1 and B-2). Trichomes and protrusions were borne on the upper epidermal cells of hull-like tissues (Fig. 2, B-3 and B-4). Figure 2C shows the hull-lodicule-pistil chimeras in *cfo1* flowers. In addition to the differentiated lodicule- and hull-like tissues, stigma-like tissues (Fig. 2, C-3 and C-4) were observed at the top of these hull-lodicule-pistil chimeras. Transverse sections of the hull-lodicule-pistil chimeras revealed the presence of inner pistil-like cell layers in the middle segment, together with silicified upper epidermal cells that resembled those of the lemma or bop, whereas lodicule-like cell layers were observed in the marginal region (Fig. 2C-5).

Most *cfo1* flowers displayed ectopic floral organs (efo) with different types of identities on the palea side of whorl 2 (Supplemental Fig. S1A), where the wild-type flowers developed no organs. Most of the efo resembled hulls with lemma- or bop-like epidermal cells (Fig. 2, D-1 and D-2). Some of the efo showed lodicule-like identity (Fig. 2C-3, red arrow). Others developed into types of chimeras, such as an ectopic hull-lodicule chimera (Fig. 2, D-3 and D-4) and ectopic hull-pistil chimera (Fig. 2, D-5–D-7).

In whorl 3, stamen number was reduced in 39% (n = 100) of the *cfo1* flowers examined (Supplemental Fig. S1A). Stamen-pistil chimeras were visualized in 16% (n = 100) of the *cfo1* flowers examined (Fig. 2E). These stamen-pistil chimeras generally consisted of a basal thick filament, middle vestigial anthers, and apical styles plus stigmas (Fig. 2, E-2–E-4), whereas the wild-type stamen was composed of a thin filament and an anther with four sacs (Fig. 2, A-1, A-3, and A-6).

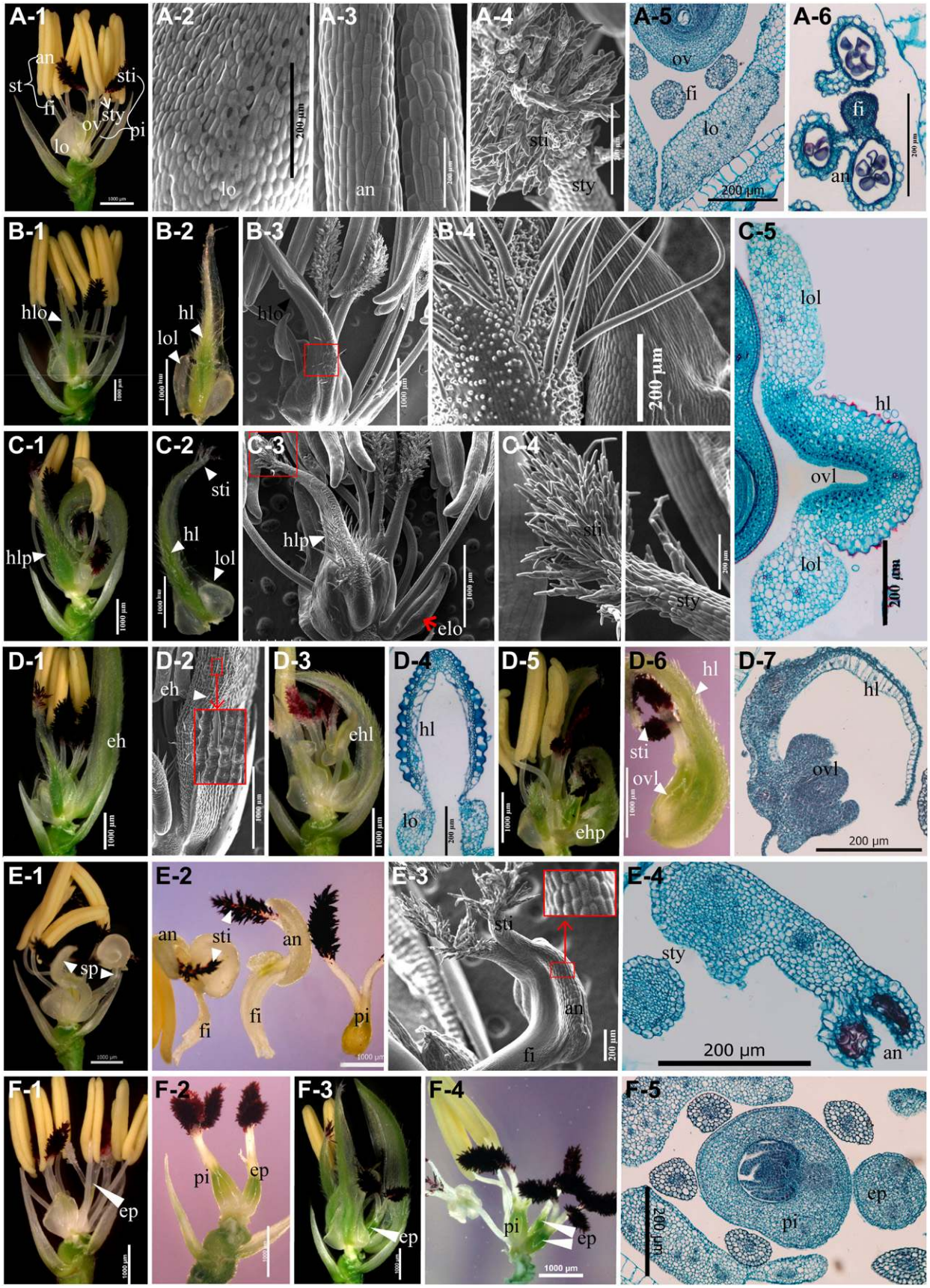

Figure 2. Inner floral organs of *cfo1* flowers. A, Inner floral organs in the wild type. A-1, A wild-type spikelet; the lemma and palea were removed. A-2 to A-4, Scanning electron micrographs of the lodicule, stamen, and stigma, respectively. A-5 and A-6,

In whorl 4, the wild-type pistil contained one ovary and bore a double-plumed stigma on a short style (Fig. 2, A-1, A-4, and A-5). In *cfo1* flowers, the pistil usually appeared morphologically normal and fertile. However, one or occasionally more additional pistils were produced at the side of the normal pistil in half of the *cfo1* flowers (Fig. 2, F-1–F-5; Supplemental Fig. S1A). The extra pistils appeared to have a normal ovary and normal stigmas, but they might fail to develop normal ovules and thus be sterile (Fig. 2F-5), given that no multiseeded spikelets were observed among the mutants.

To determine further the identities of these mutated organs, the expression levels of known floral organ development genes were determined in different organs using qRT-PCR (Supplemental Fig. S2). In *cfo1* lodicules, the A-class genes *OsMADS14* and *OsMADS15*, C-class genes *OsMADS3* and *OsMADS58*, D-class gene *OsMADS13*, E-class gene *OsMADS1*, and *DL* all showed ectopic expression. The B-class gene *OsMADS2* and the *AGL6*-like gene *OsMADS6* were expressed at lower levels than in wild-type lodicules, whereas the expression levels of two other B-class genes, *OsMADS4* and *OsMADS16*, were not obviously affected. In *cfo1* stamens, the *OsMADS58*, *OsMADS13*, *DL*, and *OsMADS6* genes showed ectopic expression, and the expression of *OsMADS2*, *OsMADS4*, and *OsMADS3* was up-regulated. The expression levels of other genes were not visibly altered. In the efo of *cfo1* flowers, all detected genes except *OsMADS58* showed a high level of expression. In *cfo1* pistils, the expression of most detected genes other than *OsMADS2* and *DL* was unaffected. These results suggest that in *cfo1* flowers, the lodicule acquired hull- and pistil-like identities, the efo acquired other types of identities, and the stamens acquired pistil-like identities. These results are consistent with the results of the phenotype analysis.

Abnormal Early Flower Development in *cfo1*

Scanning electron microscopy analysis of floral organ morphogenesis during early developmental stages was undertaken. No significant morphological differences were observed during the spikelet 5 stage (Sp5; formation of lodicule primordia; Fig. 3, A and E). During the Sp6 stage, the wild-type flower formed six hemispherical stamen primordia (Fig. 3, B and C). The stamen primordia were not observed in *cfo1* flowers (Fig. 3, F and G). Early in Sp6, no inner floral organ primordia appeared in *cfo1* flowers (Fig. 3F). Later in Sp6, two zygomorphic crescent-shaped primordia began to develop on the lemma side, where wild-type lodicule primordia develop (Fig. 3G). The efo primordia were formed on the palea side of *cfo1* flowers during this stage. At the Sp7 stage, with formation of the pistil, wild-type stamen primordia differentiated into quadrangular anthers and filaments (Fig. 3D), whereas *cfo1* flowers displayed expanding lodicule-like organ primordia in whorl 2 and hemispherical stamen primordia in whorl 3 (Fig. 3H). During Sp8, with formation of the ovules and pollen, inner floral organs underwent normal development in wild-type flowers (Fig. 3I), whereas *cfo1* flowers displayed elongated lodicules (Fig. 3J) and efo in whorl 2 (Fig. 3, K and L) and irregular-shaped organs in whorl 3 (Fig. 3, J–K). All of these results indicated that floral organ identities were altered during early flower development in *cfo1* mutants.

Effects of Mutation of *CFO1* on Expression Patterns of Floral Organ Identity Genes during Early Stages of Flower Development

To determine further the identity of chimeric organs in *cfo1*, the expression patterns of known genes for

Figure 2. (*Continued.*)
Transverse sections of the inner floral organs. B, Hull-lodicule chimeras (hlo) in cfo1 flowers. B-1, A cfo1 spikelet with a hlo (indicated by the white triangle); the lemma and palea were removed. B-2, The hlo shown in B-1. The white triangles indicate lodicule- and hull-like tissues. B-3 and B-4, Scanning electron micrographs of a hlo. B-4, Higher magnification of the portion of B-3 enclosed in the red frame. Trichomes and protrusions were observed on the epidermal cells of the hlo. B-5, Transverse section of a hlo. Hull- and lodicule-like cell structures were observed. C, Hull-lodicule-pistil chimeras (hlp) in cfo1 flowers. C-1, A cfo1 spikelet with hlp (indicated by the white triangle); the lemma and palea were removed. C-2, The hlp shown in C-1. The white triangles indicate lodicule-, hull-, and stigma-like tissues. C-3 and C-4, Scanning electron micrographs of a hlp. C-4 shows a higher power magnification of the portion of C-3 enclosed in the red frame. Stigma-like cells were observed at the top of the hlp. D, The efo in cfo1 flowers. D-1, A cfo1 spikelet with an ectopic hull (eh; indicated by white triangles); the lemma and palea were removed. D-2, Scanning electron micrographs of an eh. The large red frame shows a higher power magnification of the portion enclosed in the small red frame. D-3, A cfo1 spikelet with an ectopic hull-lodicule chimera (ehl). D-4, Transverse section of an ehl. D-5, A cfo1 spikelet with an ectopic hull-pistil chimera (ehp). D-6, The ehp shown in D-5. D-7, Transverse section of an eh. Hull- and ovary-like cell structures were observed. E, Stamen-pistil chimeras (sp) in cfo1 flowers. E-1, A cfo1 spikelet with two sp; the lemma and palea were removed. E-2, The two sp and the pistil in whorls 3 and 4 shown in E-1. E-3, Scanning electron micrograph of a sp. E-4, Transverse section of a sp. Style- and anther-like cell structures were observed. F, Extra pistils in whorl 4 of cfo1 flowers. F-1, A cfo1 flower with six stamens and two pistils; the lemma and palea were removed. F-2, A cfo1 flower with normal pistil and the extra pistil in whorl 4; the other floral organs were removed. F-3, A cfo1 flower with extra pistils; the lemma and palea were removed. F-4, One normal pistil and two extra pistils shown in F-3; the other floral organs were removed. F-5, Transverse section of a cfo1 flower with one extra pistil in whorl 4. an, Anther; fi, filament; elo, ectopic lodicule-like organ; ep, extra pistil; hl, hull-like tissue; lo, lodicule; lol, lodicule-like tissue; ov, ovary; ovl; ovary-like tissue; pi, pistil; st, stamen; sti, stigma; sty, style. Bars = 1,000 μm in A-1, B-1 to B-3, C-1 to C-3, D-1 to D-3, D-5, D-6, E-1, E-2, and F-1 to F5; bars = 200 μm in all other images.

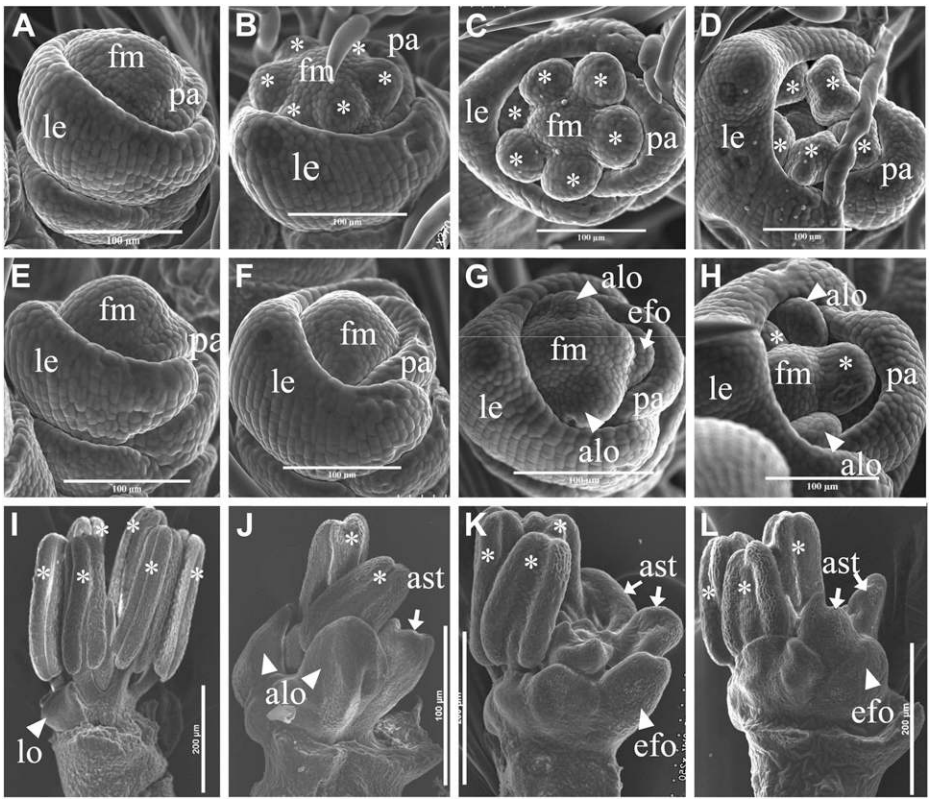

Figure 3. Scanning electron micrographs of early *cfo1* flowers. A to D, Scanning electron microscopy of wild-type flowers at stages Sp5 (A), early Sp6 (B), later Sp6 (C), and Sp7 (D). E to H, Scanning electron microscopy of *cfo1* flowers at stages Sp5 (E), early Sp6 (F), later Sp6 (G), and Sp7 (H). F to H show delayed initiation of stamen primordia. Abnormal lodicule primordia were observed in G and H, and efo primordia were observed in G. I, Inner floral organs during stage Sp8 in a wild-type flower. J to L, Inner floral organs during stage Sp8 in *cfo1* flowers. Abnormal lodicules were observed in J, and efo and abnormal stamens were observed in K and L. alo, Abnormal lodicule; ast, abnormal stamen; fm, floral meristem; le, lemma; lo, lodicule; pa, palea. Bars = 100 μm in A to H and 200 μm in I to L.

floral organ identity were investigated during early stages of flower development (stages Sp5–Sp8) with in situ hybridization.

During stages Sp5 to Sp7, *OsMADS6* expression was detected in precursor cells and primordia of the mrp, lodicule, and pistil of both wild-type (Fig. 4, A-1–A-3) and *cfo1* (Fig. 4, B-1–B-3) flowers. However, abnormal expression was detected in transverse sections of Sp8 flowers. In the *cfo1* mrp, the *OsMADS6* expression signal decreased gradually from the lateral vascular bundle to the margin (blue triangles in Fig. 4, B-4 and B-5), whereas its expression was uniformly distributed in the wild-type mrp (arrows in Figure 4, A-4 and A-5). In potential *cfo1* hull-pistil-lodicule chimeras, *OsMADS6* was only expressed in both marginal tissues (potential lodicule tissues) and not in the central portion containing potential hull tissues (red triangles in Fig. 4B-4). In some efo, an obvious *OsMADS6* expression signal was detected (yellow triangles in Fig. 4, B-4 and B-5).

Expression signals of the B-class genes *OsMADS2*, *OsMADS4*, and *OsMADS16* were detected in the lodicules and stamens of both wild-type and *cfo1* flowers during stages Sp5 to Sp8 (Fig. 4, B-1–H-5). However, differences between wild-type and *cfo1* flowers were obvious. In longitudinal sections of Sp6- and Sp7-stage *cfo1* flowers, *OsMADS2* and *OsMADS16* signals were absent in parts of the lodicule primordium (red triangles in Fig. 4, D-2, D-3, H-2, and H-3). In transverse sections of Sp6- and Sp7-stage *cfo1* flowers, *OsMADS2*, *OsMADS4*, and *OsMADS16* signals were absent in the central region of hull-pistil-lodicule chimeras of *cfo1* flowers, whereas signals were detected in both sides of these organs (red triangles in Figure 4, D-4, F-4, and H-4). In addition, *OsMADS16* was only expressed in potential stamen tissues of *cfo1* stamen-pistil chimeras (green triangles in Fig. 4, H-3 and H-5). The *OsMADS2* and *OsMADS4* genes were expressed in efo that carried potential lodicule tissues (yellow triangles in Fig. 4, D-4 and F-4) but not in ectopic hull organs (yellow triangles in Fig. 4, D-5 and F-5).

After stage Sp5, strong *OsMADS1* expression was detected in the lemma and bop, whereas a weak *OsMADS1* expression signal was detected in the mrp and pistil in wild-type flowers (Fig. 5, A-1–A-5). However, in *cfo1* flowers, *OsMADS1* was expressed in the mrp (blue triangles in Fig. 5, B-2 –B-5) and ectopic hull-like organ (yellow triangle in Fig. 5B-4), with a similar level of signal detected in the lemma and bop (Fig. 5, B-1–B-5). In addition, a distinct expression signal was detected in the central regions (potential hull tissues) of hull-pistil-lodicule chimeras in *cfo1* flowers during stage Sp8 (red triangle in Fig. 5B-5), whereas expression was difficult to detect in wild-type lodicules and pistils at the same stage (Fig. 5, A-4 and A-5).

Two C-class genes, *OsMADS3* and *OsMADS58*, were expressed in incipient cells and primordia of the stamens and pistil in both wild-type and *cfo1* flowers during stages Sp5 to Sp8 (Fig. 5, B-1–F-5). However, ectopic expression signals in abnormal lodicules were detected in longitudinal sections of Sp6- and Sp7-stage *cfo1* flowers (red triangles in Fig. 5, D-2, F-2, and F-3). The ectopic expression signal was observed in partial

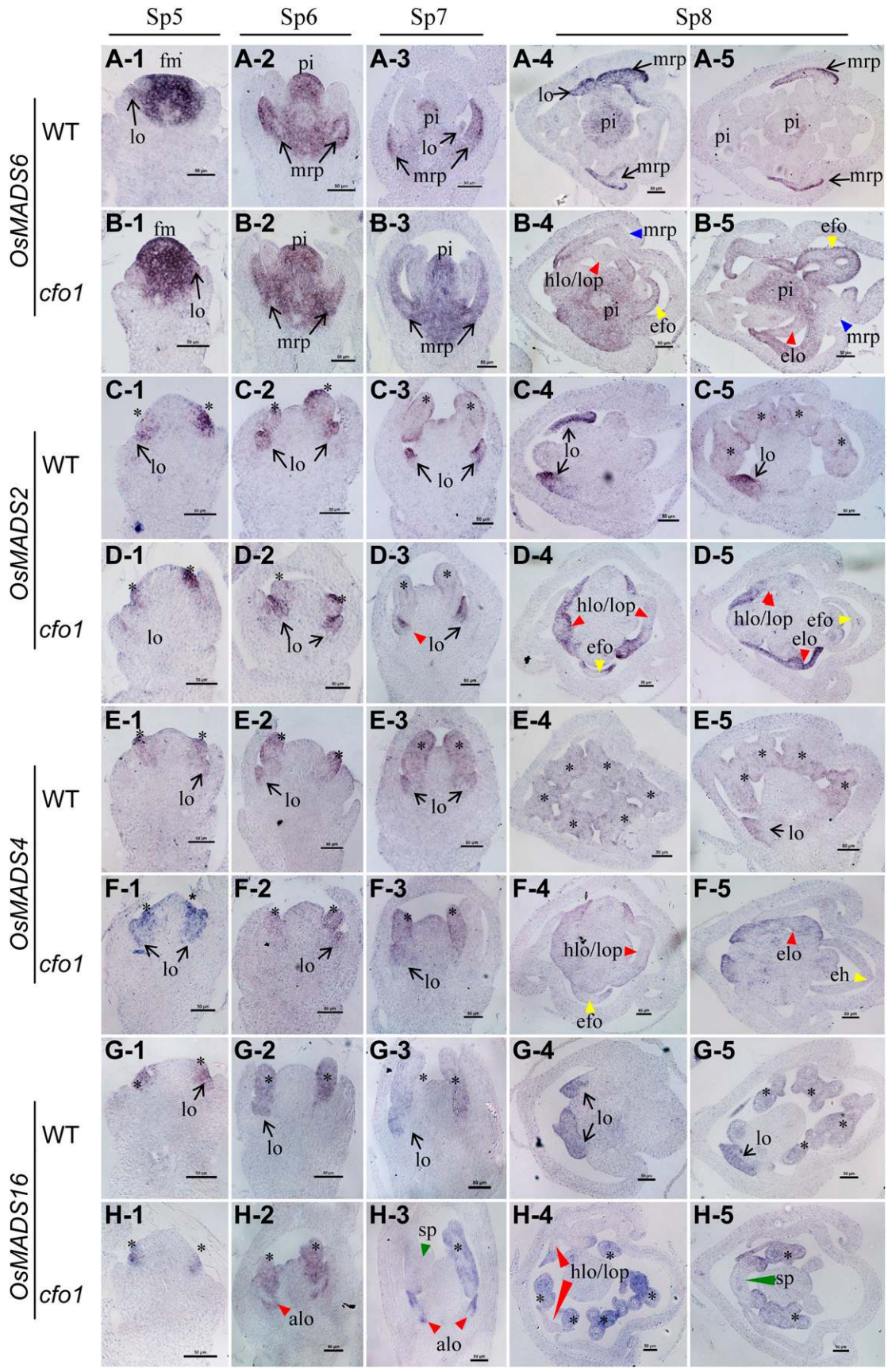

Figure 4. *OsMADS6* and B-class gene expression in *cfo1* and wild-type flowers at early stages of development of *cfo1* flowers. Expression of *OsMADS6* (A), *OsMADS2* (C), *OsMADS4* (E), and *OsMADS16* (G) is shown in wild-type flowers, and expression

regions (potential pistil tissues) of hull-pistil-lodicule chimeras of Sp8-stage *cfo1* flowers (red triangles in Fig. 5, D-4, D-5, F-4, and F-5). The D-class gene *OsMADS13* was expressed in ovule primordia in both wild-type and *cfo1* flowers during stages Sp6 to Sp8 (Fig. 5, D-4, D-5, F-4, and F-5). However, an ectopic *OsMADS13* expression signal was detected in lower layer cells (potential ovary tissues) of the central portion of hull-pistil-lodicule chimeras of *cfo1* flowers at the Sp8 stage (Fig. 5, H-3 and H-4).

During stages Sp5 to Sp6, *DL* expression was only detected in lemma primordia (arrow in Fig. 6A) and not in pistil incipient cells or primordia in wild-type flowers (Fig. 6, A and D). Ectopic expression signals of *DL* were detected in abnormal mrp (blue triangles in Fig. 6, B and E) and abnormal lodicule primordia (red triangles in Fig. 6, C and F) in *cfo1* flowers. During the Sp7 stage, *DL* was expressed in pistil primordia in wild-type (arrow in Fig. 6G) and *cfo1* (arrows in Fig. 6, H and I) flowers. In addition, *DL* expression was detected in abnormal primordia of mrp, efo, and stamens (triangles in Fig. 6, H and I) in *cfo1* flowers. During the Sp8 stage, *DL* expression was observed in the peripheral domain of the medial vascular bundle of the lemma (arrows in Figure 6, J and K) and the pistil (arrows in Fig. 6, M–O) in wild-type and *cfo1* flowers. In addition, strong *DL* transcription signals in *cfo1* flowers were detected in the peripheral domains of lateral vascular bundles of the palea (blue triangles in Fig. 6, K and L), the peripheral domains of the vascular bundle of ectopic hull-like organs (yellow triangles in Fig. 6, K and O), central regions of hull-pistil-lodicule chimeras (red triangles in Fig. 6L), and stamen-pistil chimeras (green triangles in Fig. 6, N and O).

In the *cfo1* mrp, the ectopic expression of *DL*, increased expression of *OsMADS1*, and decreased expression of *OsMADS6* implied that the *cfo1* mrp primordia developed a lemma identity at an early stage of flower development. In the *cfo1* lodicule, the ectopic expression of *DL*, *OsMADS1*, and C/D-class genes, and the lack of expression of *OsMADS6* and B-class genes, suggested that *cfo1* lodicules acquired hull and pistil identities in the primordial development stage. The ectopic expression of *DL* and *OsMADS13* in *cfo1* stamen primordia implied that pistil-like tissues were produced in whorl 3 at an early stage of flower development. In particular, we noted that *DL* is expressed ectopically throughout all of the abnormal floral organs in early-stage *cfo1* flowers during the initiation and formation of organ primordia. Thus, we speculated that the expression of *DL* is probably regulated negatively by *CFO1*.

CFO1 Encodes OsMADS32, a MADS-Box Protein

A map-based cloning strategy was used to isolate the *CFO1* gene. Genetic analysis demonstrated that the *cfo1* trait was controlled by a single recessive gene (Supplemental Table S1). The *cfo1* locus was mapped on the short arm of chromosome 1 within an approximately 645-kb region between the simple sequence repeat markers RM1152 and RM128 (Fig. 7, A and B). Fortunately, a gene that encodes a 196-residue MADS box transcription factor, OsMADS32, occurs in this region. Sequence comparison revealed that *OsMADS32* in the *cfo1* mutant was missing a single nucleotide (T) at position 214 of the open reading frame, which caused a premature translation stop (Fig. 7, C and D). An *Rsa*I restriction site in the wild-type allele was abolished in the *cfo1* mutant allele because of this single-nucleotide deletion (Fig. 7C). A cleavage amplification polymorphism site (CAPS) marker was designed to distinguish the wild-type and mutant alleles in the segregating population. Results of *Rsa*I digestion of PCR products suggested significant cosegregation of the CAPS marker with the *cfo1* allele (Supplemental Fig. S3).

Complement testing was conducted as follows. First, *OsMADS32* overexpression plants (*M32OE*) that expressed *OsMADS32* under the control of the cauliflower mosaic virus 35S promoter in the *japonica* rice 'Zhonghua11' were generated. These plants displayed no defects except reduced palea size (Supplemental Fig. S4). Next, we crossed the *cfo1* mutant with *M32OE* homozygotes. Six F1 individuals with the *M32OE* phenotype were planted to generate F2 populations, and a 3:12:1 (normal phenotype:*M32OE* phenotype: *cfo1* mutant phenotype) ratio was observed in these F2 plants (Supplemental Table S2). The genotypes of 25 random F2 lines were identified using two specific molecular markers. Four *M32OE_cfo1cfo1* lines showed normal floral organ development, except for reduced palea size (Fig. 7, E–G). This indicated that *OsMADS32* expression in the *cfo1* mutant background can recreate the *cfo1* phenotype. In addition, we identified one T-DNA insertion line at the *OsMADS32* locus (no. 05Z11AF36 [AF36]) from the Rice Mutant Database. In AF36, the T-DNA insertion resulted in severe DNA recombination of *OsMADS32* genome sequences from

Figure 4. (*Continued.*)
of OsMADS6 (B), OsMADS2 (D), OsMADS4 (F), and OsMADS16 (H) is shown in cfo1 flowers. Rows 1 to 3 show longitudinal sections of flowers at stages Sp5 to Sp7, respectively, and rows 4 and 5 show transverse sections of flowers at the Sp8 stage. Black arrows indicate normal gene expression in the lodicules or mrp. Asterisks indicate normal gene expression in the stamens. Blue, red, yellow, and green triangles indicate abnormal gene expression in the mrp, abnormal lodicule/hull-lodicule chimera/lodicule-pistil chimera, efo, and stamen-pistil chimera, respectively. alo, Abnormal lodicule; eh, ectopic hull-like organ; elo, elongated lodicule; fm, floral meristem; hlo, hull-lodicule chimera; lo, lodicule; lop, lodicule-pistil chimera; pi, pistil; sp, stamen-pistil chimera. Bars = 50 μm.

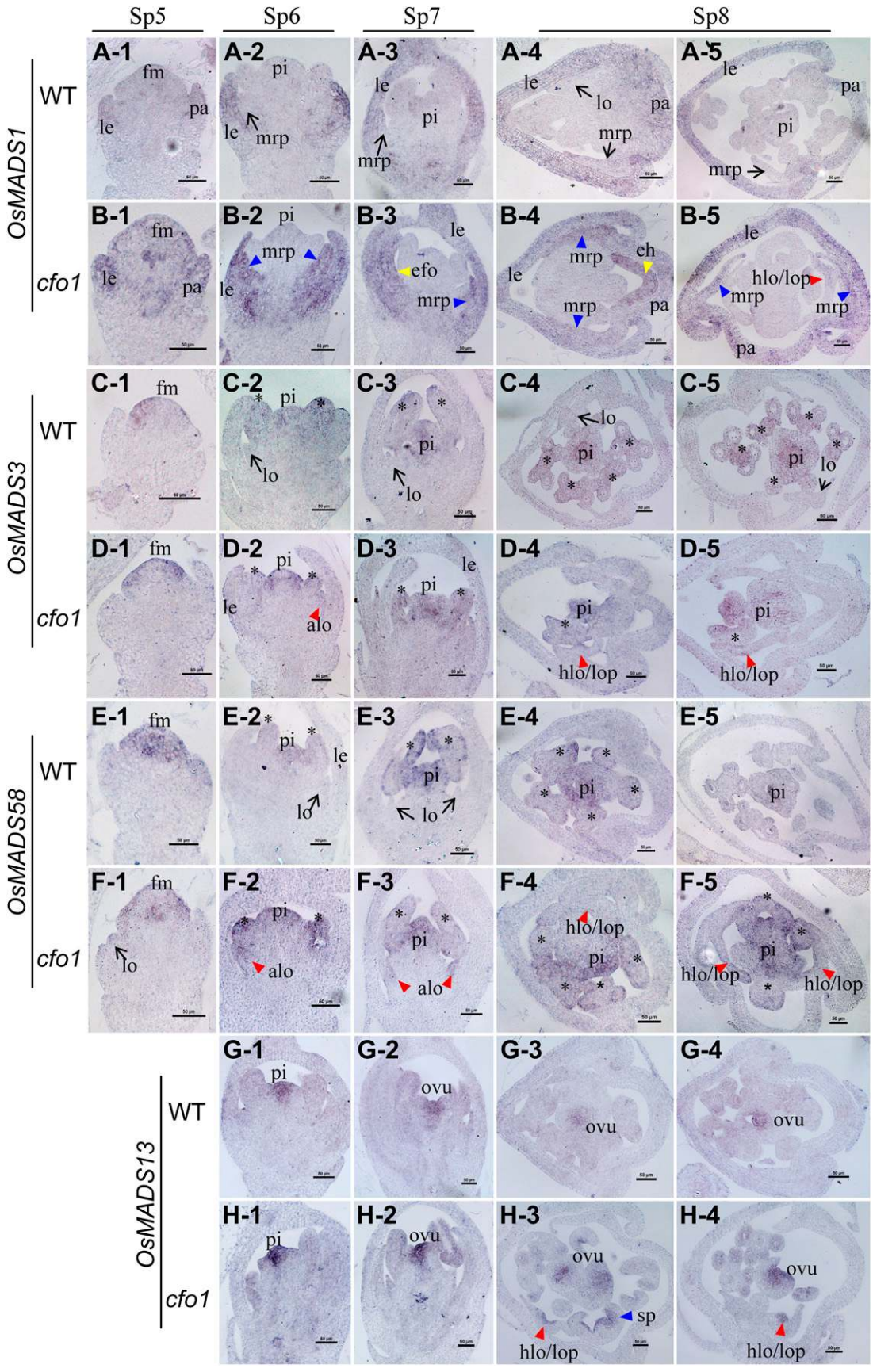

Figure 5. Expression of *OsMADS1* and C- and D-class genes in *cfo1* and wild-type flowers at early stages of flower development. Expression of *OsMADS1* (A), *OsMADS3* (C), *OsMADS58* (E), and *OsMADS13* (G) is shown in wild-type flowers, and

−157 bp (upstream promoter) to 363 bp (the second exon; Fig. 7C; Supplemental Fig. S5, A–C; Zhang et al., 2006). This suggested that AF36 is a complete loss-of-function mutant of *OsMADS32*. Next, allelic verification between AF36 and *cfo1* was performed. F1 individuals derived from the cross between *cfo1* and AF36 were identified (Supplemental Fig. S5, D and E). The *cfo1*, AF36, and F1 progeny displayed very similar flower phenotypes (Supplemental Fig. S5F), which indicated that *cfo1* and AF36 are allelic. Taken together, these results demonstrated that *CFO1* and *OsMADS32* are the same gene.

CFO1 Belongs to a Monocot-Specific Class

The MIKC-type genes are classified as a plant-specific subfamily of the MADS box gene family. This subfamily contains a well-conserved MADS (M) domain and three additional plant-specific domains: an intervening (I) domain, a keratin-like coiled-coil (K) domain, and a C-terminal (C) domain (Theissen et al., 1996; Alvarez-Buylla et al., 2000). The MIKC-type genes can be further divided into two subgroups, $MIKC^C$ and MIKC*, based on the intron-exon structure. Although OsMADS32/CFO1 is indicated to be a typical $MIKC^C$-type protein, its phylogenetic relationships remain unclear (Ma et al., 1991; Nam et al., 2004; Arora et al., 2007).

We constructed a phylogenetic tree with 153 selected MIKC protein sequences from clubmosses, mosses, basal angiosperms, core eudicots, and monocots, including several genome-sequenced species, such as Arabidopsis, soybean (*Glycine max*), *Medicago truncatula*, poplar (*Populus trichocarpa*), *Phoenix dactylifera*, grape (*Vitis vinifera*), rice, *Sorghum bicolor*, and maize (Fig. 8). The 153 $MIKC^C$-type genes were divided into 13 distinct classes: A or AP1-like class (A-AP1), B-AP3, B-PI, Bs-TT16, C/D-AG, E-SEP, F-SOC1, T-SVP, AGL6-like, AGL12-like, ANR1-like, FLC-like, and CFO1-like (Fig. 8). Interestingly, CFO1 and its orthologs from grasses and *P. dactylifera* constituted the earliest diverging CFO1-like class in the $MIKC^C$ family (Fig. 8). This class included Pd from *P. dactylifera*, TaAGL14 and TaAGL15 from wheat, ZmMADS32 and ZmLOC100279931 from maize, HvWM16 from barley, Sb03g03380 from *S. bicolor*, Bd12g48690 from *Brachypodium distachyon*, and CFO1 from rice (Fig. 8). These results suggest that the CFO1-like gene class is monocot specific.

Sequence analysis indicated that CFO1-like proteins are well conserved, except that Sb03g03380 contains a distinct C domain (Supplemental Fig. S6). Although the M and K domains were conserved in other $MIKC^C$-type proteins, CFO1-like proteins possessed some unique sites (Ser-6, Ser-19, Asp-26, and Phe-29) and motifs ($DLLLLL^{42–47}$ and $MTVDDG^{109–114}$) in these two domains (Supplemental Fig. S6). In addition, distinct differences were observed in the I and C domains across all classes (Supplemental Fig. S6).

Temporal and Spatial Expression Patterns of *CFO1*

As already described, the expression of defective *CFO1* disturbs floral organ identities in rice. To determine the pattern of *CFO1* expression, semiquantitative reverse transcription (RT)-PCR and qRT-PCR analysis were conducted. No *CFO1* transcripts were detectable in vegetative organs, namely roots, stems, or leaves (Fig. 8A). However, *CFO1* transcription was observed in inflorescences at stages 1 to 7 (Fig. 9, B and C). After inflorescence stage 6, when the floral organs start to differentiate, *CFO1* transcription levels decreased gradually (Fig. 9, B and C).

We investigated *CFO1* expression in wild-type plants using in situ hybridization. The *CFO1* gene was expressed initially in the primary and secondary branch meristems (Fig. 9D). Abundant *CFO1* transcripts were detected subsequently in the meristems of spikelets and florets (Fig. 9, E and F). During stages Sp6 and Sp7, when the stamen primordia were initiated, analysis of serial longitudinal and transverse sections indicated that the expression signals of *CFO1* were focused on several specific domains and organs (Fig. 9, G–K). First, *CFO1* was expressed strongly in organ primordia, such as rudimentary glumes (Fig. 9, G and H), the mrp (lines in Fig. 9, I–K), lodicules (triangles in Fig. 9, G, H, and L), upper and central regions of stamens (asterisks in Fig. 9, I–K), and the upper region of the pistil (Fig. 9, G–K). Second, *CFO1* was expressed in vascular bundles of floral organ primordia, such as the rachilla (arrows in Fig. 9G), sterile lemma (arrows in Fig. 6I), and lemma and palea (arrows in Fig. 9, I–K), which are normal in *cfo1* flowers. During stage Sp8, *CFO1* was expressed at high levels in the lodicules and rudimentary glumes and at low levels in the stamens and pistils (Fig. 9L). Although *CFO1* function was not obvious in rudimentary glumes and vascular bundles, the data strongly suggested that *CFO1* expression was associated with its function in floral organ specification.

Figure 5. (*Continued.*)
expression of OsMADS1 (B), OsMADS3 (D), OsMADS58 (F), and OsMADS13 (H) is shown in cfo1 flowers. Rows 1 to 3 show longitudinal sections of flowers at stages Sp5 to Sp7, respectively, and rows 4 and 5 show transverse sections of flowers at the Sp8 stage. Black arrows indicate normal gene expression in the lodicules or mrp. Asterisks indicate normal gene expression in stamens. Blue, red, and yellow triangles indicate abnormal gene expression in the mrp, abnormal lodicule/hull-lodicule chimera/lodicule-pistil chimera, and efo, respectively. alo, Abnormal lodicule; eh, ectopic hull-like organ; fm, floral meristem; hlo, hull-lodicule chimera; le, lemma; lo, lodicule; lop, lodicule-pistil chimera; ovu, ovule; pa, palea; pi, pistil; sp, stamen-pistil chimera. Bars = 50 μm.

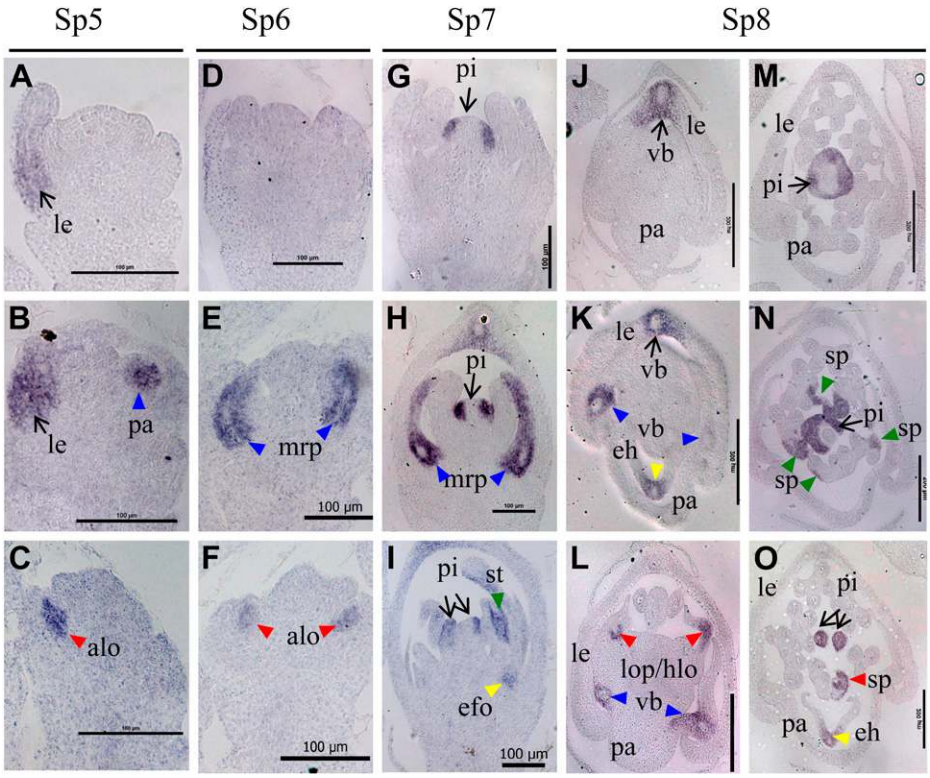

Figure 6. Expression of *DL* during early stages of development of *cfo1* and wild-type flowers. Expression in flowers at the Sp5 (A–C), Sp6 (D–F), Sp7 (G–I), and Sp8 (J–O) stages in wild-type flowers (A, D, G, J, and M) and *cfo1* flowers (B, C, E, F, H, I, K, L, N, and O) is shown. The domain of *DL* expression in the lemma and pistil is indicated by arrows, whereas its ectopic expression in other organs is indicated by triangles. Blue, red, yellow, and green triangles indicate the expression domain in abnormal palea/mrp, lodicule, efo, and stamens, respectively. alo, Abnormal lodicule; eh, ectopic hull-like organ; hlo, hull-lodicule chimera; le, lemma; lo, lodicule; lop, lodicule-pistil chimera; pa, palea; pi, pistil; sp, stamen-pistil chimera; vb, vascular bundle. Bars = 100 μm in A to I and 200 μm in J to O.

Genetic Interactions between *CFO1* and *DL*

The expression pattern analysis indicated that CFO1 negatively regulates *DL* expression. In order to examine the genetic interactions between *CFO1* and *DL*, we generated *cfo1+dl-sup1* double mutants and analyzed the phenotypes of their floral organs.

The *dl-sup1* mutant is a loss-of-function mutant in which *DL* expression is not observed at any stage of flower development (Yamaguchi et al., 2004). The lemma and pistil in *cfo1+dl-sup1* flowers displayed similar phenotypes to those of *dl-sup1* flowers but not those of *cfo1* flowers. The lemma is smaller than the palea (Fig. 10, A and B), and the pistil is transformed into stamen-like organs or repeat lodicule- and stamen-like structures in both *cfo1+dl-sup1* and *dl-sup1* flowers (Fig. 10, G and H), whereas the lemma and pistil identities in *cfo1* flowers showed no obvious changes compared with the wild type (Figs. 1B and 2E-2). Therefore, the phenotypes of the lemmas and pistils in *cfo1+dl-sup1* flowers were as expected. However, interesting changes were found in the mrp, lodicules, efo, and stamens of each *cfo1+dl-sup1* flower. First, the palea showed a normal phenotype in *cfo1+dl-sup1* flowers because the mrp possessed normal identity (Fig. 10, D and F), whereas a lemma-like identity was exhibited in the *cfo1* mrp (Fig. 1, B and D). Second, the *cfo1+dl-sup1* flowers had elongated lodicules but no hull- or pistil-like tissues (Fig. 10, H, J, and L), whereas *cfo1* flowers showed hull- and pistil-like lodicules in whorl 2 (Fig. 2, B and C). Third, although efo were still produced in whorl 2 on the palea side of *cfo1+dl-sup1* flowers, all of these appeared to be identical to lodicules (Fig. 10, J and M). In the *cfo1* flowers, hull- and pistil-like tissues were also observed in efo, together with lodicule-like tissues (Fig. 2D). Finally, no stamen-pistil chimeras were found in whorl 3 of *cfo1+dl-sup1* flowers, although they often occurred in *cfo1* flowers (Fig. 2E). Therefore, these results indicated that *DL* inactivation reverses the defects seen in *cfo1* floral organs. Given the ectopic expression of *DL* in *cfo1* flowers, these results suggested that *DL* activation was an important cause of the defective mrp and ectopic formation of hull- and pistil-like tissues in whorls 2 and 3.

The expression levels of known genes for floral organ development were analyzed in *cfo1* and *cfo1+dl-sup1* floral organs during the heading stage (Fig. 10, N–P). The *OsMADS14* and *OsMADS3* genes maintained expression levels comparable to those of the ectopically expressed genes in *cfo1* lodicules. However, compared with *cfo1* lodicules, the expression of *OsMADS58* and *OsMADS13* was drastically decreased in *cfo1+dl-sup1* lodicules, whereas the expression of *OsMADS2* and *OsMADS16* was drastically increased. Expression of *OsMADS1* was not detected in *cfo1+dl-sup1* lodicules but was clearly evident in *cfo1* lodicules. Compared with the ectopically expressed genes in the *cfo1* efo, *OsMADS14*, *OsMADS15*, *OsMADS13*, *OsMADS1*, and *OsMADS6* showed clearly decreased expression in the *cfo1+dl-sup1* efo. Absent or diminished expression of these genes, which control hull and pistil development, may result in *cfo1+dl-sup1* lodicules and efo that lack hull- and pistil-like identities. This conclusion is consistent with the results of the phenotype analysis.

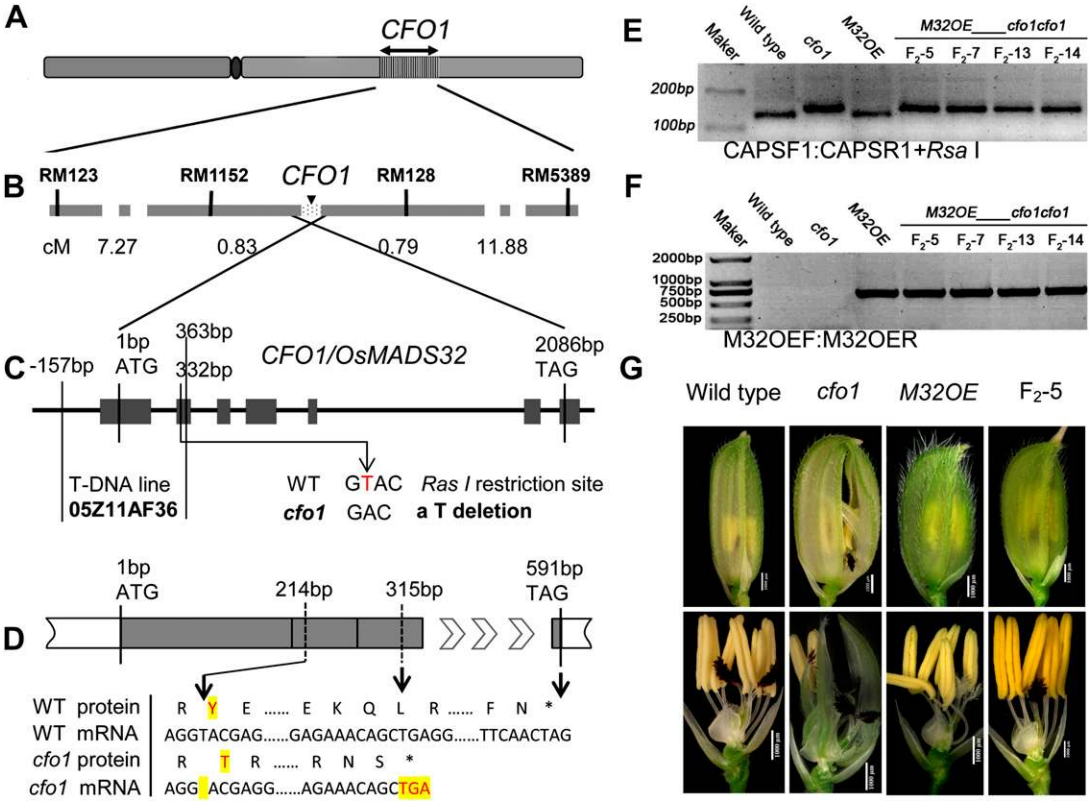

Figure 7. Map-based cloning of *CFO1*. A, Location of *CFO1* on chromosome 1. B, Fine-mapping of the *CFO1* locus. C, Genomic structure of *CFO1/OsMADS32*. The site of the mutation in *cfo1* and the T-DNA insertion site of AF36 are shown. The *cfo1* mutation lies within an *Rsa*I restriction site. D, The *cfo1* mutation caused a premature translation stop. E, Verification of the *cfo1* mutation site in the F2 progeny of *cfo1* and *M32OE* plants using a CAPS marker. F, Verification of the *M32OE* site in the F2 progeny of *cfo1* and *M32OE* plants using specific markers. G, Flower phenotypes of wild-type, *cfo1*, *M32OE*, and F2 progeny with genotype *M32OE_cfo1cfo1*. WT, Wild type. Bars = 1,000 μm in G. [See online article for color version of this figure.]

We also investigated floral organ morphogenesis in *cfo1+dl-sup1* and *dl-sup1* flowers during early developmental stages. During stages Sp6 and Sp7, the *dl-sup1* and wild-type flowers were characterized by six spherical stamen primordia (Fig. 3, C and D; Supplemental Fig. S7, B and C), whereas the initiation and development of stamen primordia in *cfo1+dl-sup1* (Supplemental Fig. S7, D–F) occurred later than in *dl-sup1* and the wild type. The stamen primordia in *cfo1+dl-sup1* resembled those of *cfo1* flowers (Fig. 3, F–H). In addition, similar to *cfo1*, the *cfo1+dl-sup1* mutant exhibited expanding lodicule-like primordia and efo primordia in whorl 2 (Fig. 3G; Supplemental Fig. S7, D–F). Therefore, these results suggested that the occurrence of ectopic organs, lodicule elongation, and delay in the development of the stamen primordia were not dependent on ectopic *DL* activation.

DISCUSSION

CFO1 Is an Important Regulator of Floral Organ Identity in Rice

The rice floret consists of one lemma, one palea, two lodicules, six stamens, and one central pistil that contains one ovule. The lemma, palea, and lodicule are monocot-specific organs, whereas the stamen, pistil, and ovule are highly conserved across all angiosperms (Kellogg, 2001). In this study, map-based cloning and functional characterization demonstrated that *CFO1*, a monocot-specific MIKC^C-type gene, is a key regulator in the specification of palea and lodicule identities in rice. Several important genes for floral organ identity have been characterized in rice. The *SEP*-like gene *OsMADS1* is required for determination of the identities of the lemma and palea (Jeon et al., 2000; Agrawal et al., 2005; Prasad et al., 2005; Chen et al., 2006). The B-class gene *OsMADS16*, C-class genes *OsMADS3* and *OsMADS58*, and D-class gene *OsMADS13* play critical roles in the specification of stamen and pistil/ovule identities (Nagasawa et al., 2003; Yamaguchi et al., 2006; Dreni et al., 2007). Recently, the *AGL6*-like gene *OsMADS6/MOSAIC FLORAL ORGANS1* was shown to specify palea, lodicule, and stamen identities (Ohmori et al., 2009; Li et al., 2010). All of these genes are MIKC^C-type members of the MADS box gene family. The B-, C-, and D-class genes mainly specify conserved organs, whereas the *OsMADS1*, *OsMADS6*, and *CFO1* genes determine grass-specific organs.

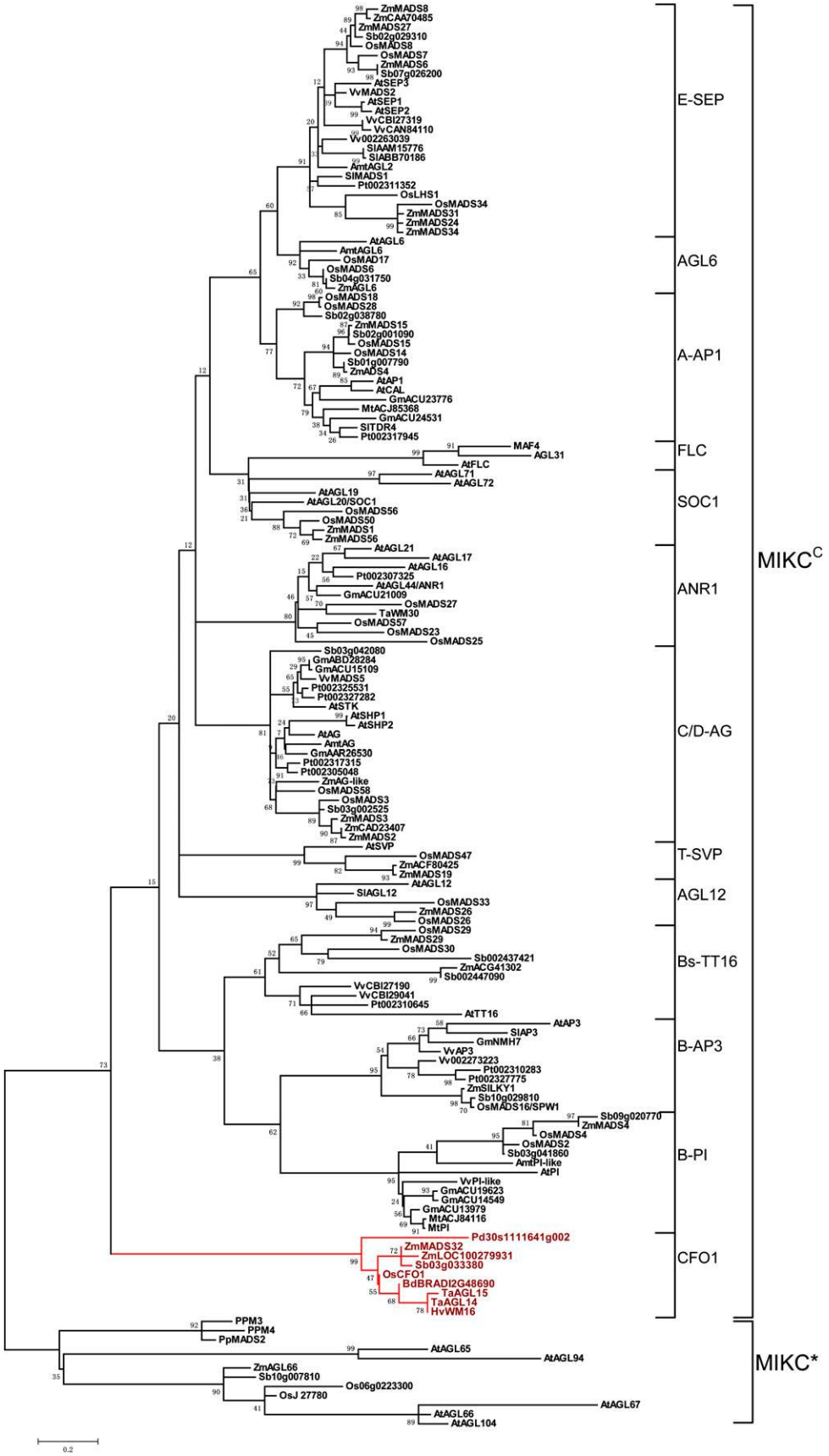

Figure 8. Evolutionary relationships among 153 MIKC genes. The phylogenetic tree was constructed using the maximum likelihood method based on the Jones-Taylor-Thornton matrix-based model. The tree was rooted using 12 MIKC*-type genes as the outgroup. Simplified class names were used (Nam et al., 2004) except for the CFO1 class. Species names are abbreviated as follows. Mosses: *Physcomitrella patens* (Pp); clubmosses: *Lycopodium annotinum* (La); basal angiosperm: *Amborella trichopoda* (Amt); eudicots: Arabidopsis (At), soybean (Gm), *M. truncatula* (Mt), poplar (Pt), grape (Vv); monocots: *P. dactylifera* (Pd), *B. distachyon* (Bd), wheat (Ta), rice (Os), barley (Hv), *S. bicolor* (Sb), maize (Zm). [See online article for color version of this figure.]

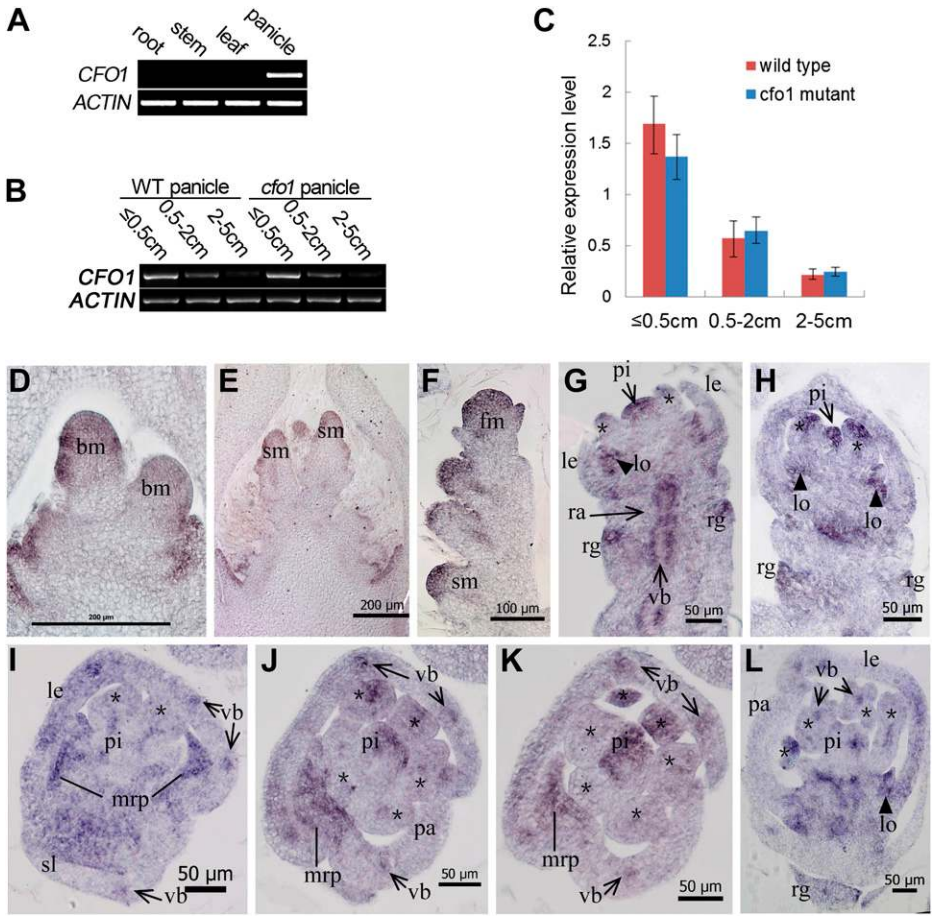

Figure 9. Expression pattern of *CFO1*. A, *CFO1* expression in different tissues as shown by RT-PCR. B, RT-PCR analysis of *CFO1* in developing wild-type (WT) and *cfo1* panicles at different stages. C, qRT-PCR analysis of *CFO1* in developing wild-type and *cfo1* panicles at different stages. D to L, In situ hybridization in wild-type panicles and flowers using a *CFO1* antisense probe. Transcription of *CFO1* was detected in the inflorescence meristem (D and E), spikelet (F), and florets (G–L) at an early development stage. Serial longitudinal sections of one floret are shown in G and H, and serial transverse sections of a different floret are shown in I to K. Asterisks in G to L indicate stamens. bm, Branch meristem; fm, flower meristem; le, lemma; lo, lodicule; pa, palea; pi, pistil; rg, rudimentary glume; sm, spikelet meristem; st, stamen; vb, vascular bundle. Bars = 200 μm in D and E, 100 μm in F, and 50 μm in G to L.

CFO1 Is Required for mrp Identity

In grass flowers, the palea and lemma are thought to have different origins (Kellogg, 2001). The palea is considered to be homologous to the prophyll (the first leaf produced by the axillary meristem), which is formed on a floret axis, whereas the lemma corresponds to the bract (the leaf that subtends the axillary meristem), which is formed on a spikelet axis (Kellogg, 2001; Ohmori et al., 2009). However, some evidence indicates that the rice palea might be derived from fusion of the mrp and bop. First, the cellular structure of the palea is very similar to that of the lemma in the body region but is distinct from that of the lemma in the marginal region (Fig. 1I; Prasad et al., 2005). Second, in plants with nonfunctional B-class genes, lodicules are transformed into organs that resemble the mrp but not the bop. Moreover, Arabidopsis plants with a mutated B class undergo homeotic transformation of petals (equivalent to lodicules) into sepals (Nagasawa et al., 2003; Yadav et al., 2007; Yao et al., 2008). This finding suggests that only the mrp, and not the whole palea, is equivalent to the sepal. In this study, the mrp of *cfo1* developed a lemma- or bop-like identity, and *CFO1* was expressed abundantly in the wild-type mrp. Recent studies have shown that *OsMADS6* is also expressed predominantly in the mrp, and mutations in *OsMADS6* lead to conversion of the mrp into lemma- or bop-like structures (Ohmori et al., 2009; Li et al., 2010). These results suggest that *CFO1* and *OsMADS6* confer important functions in the regulation of mrp identity but not bop identity. In accordance with these studies, we speculate that the mrp, bop, and lemma are equivalent to the sepal, prophyll, and bract, respectively.

In addition, in rice with the mutations *depressed palea1* (*dp1*) and *osmads15/dep*, the bop is lost or depressed, whereas the mrp remains (Luo et al., 2005; Wang et al., 2010; Jin et al., 2011). Therefore, it is likely that *CFO1* and *OsMADS6* are required for the determination of mrp identity, and *DP1* and *OsMADS15/DEP* might be involved in the regulation of bop identity. However, differences in the mrp phenotype occur between *cfo1* and *osmads6* flowers. In *osmads6* flowers, the vascular bundle forms in the broadened mrp (Ohmori et al., 2009; Li et al., 2010). Analysis of *osmads6* mutant flowers using RT-PCR indicated that *DL* is expressed ectopically in the lemma-like palea at the heading stage (Ohmori et al., 2009). Further study using in situ hybridization showed that *DL* is expressed in the midrib of palea in *osmads6* mutant flowers (Li et al., 2011a). These results suggested that homeotic conversion of the palea into the lemma

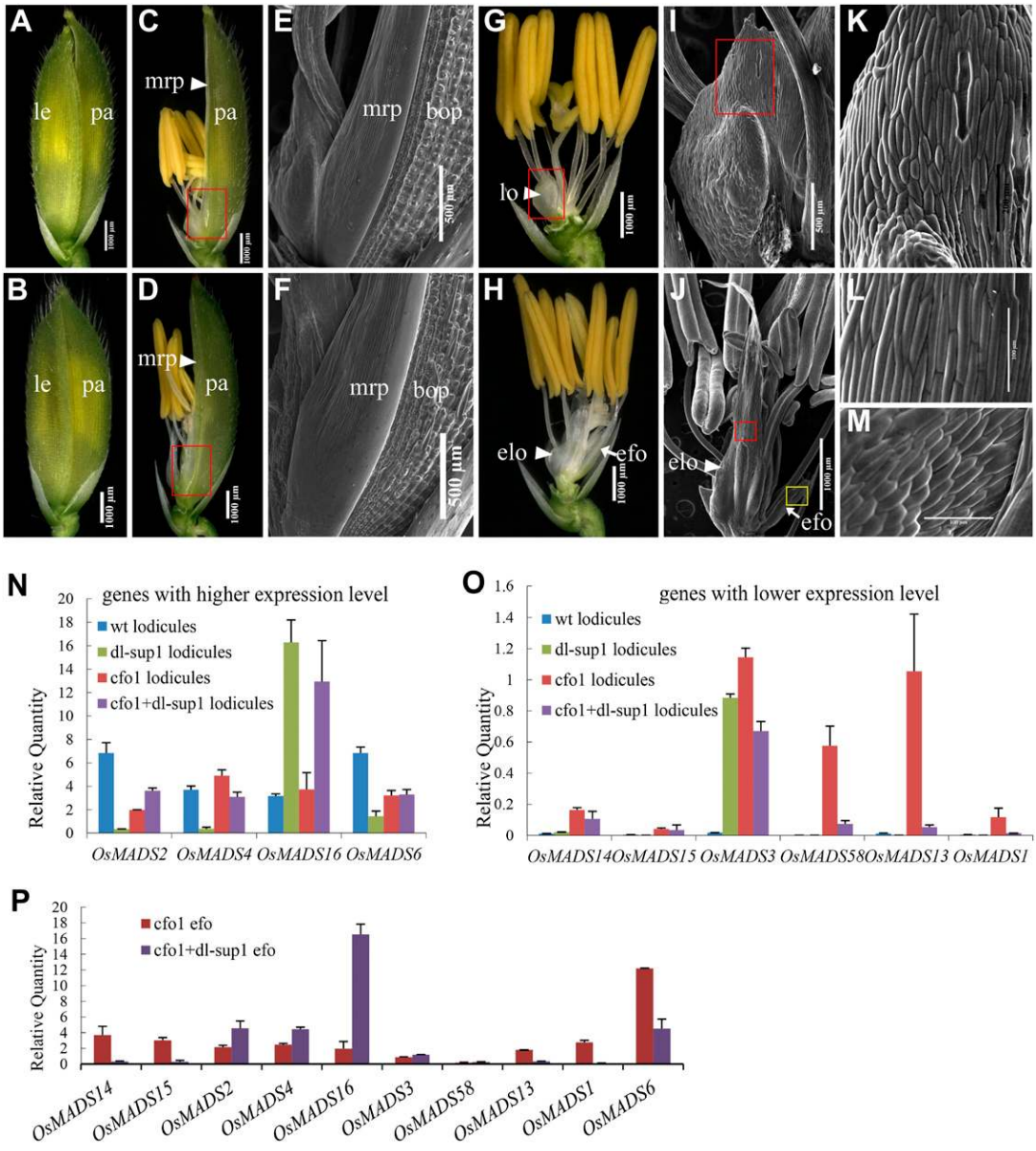

Figure 10. Phenotypes of *dl-sup1* and *dl-sup1+cfo1* flowers at the heading stage. A and B, Spikelet of *dl-sup1* (A) and *dl-sup1+cfo1* (B). C and D, Spikelet of *dl-sup1* (C) and *dl-sup1+cfo1* (D); the lemma has been removed. E and F, Scanning electron micrographs of the mrp in *dl-sup1* (E) and *dl-sup1+cfo1* (F). G and H, Spikelet of *dl-sup1* (G) and *dl-sup1+cfo1* (H); the lemma and palea have been removed. In H, elongated lodicules and efo are indicated by triangles and arrows, respectively. I and J, Scanning electron microscopy of lodicule in a *dl-sup1* flower (I) and elongated lodicule and efo in a *dl-sup1+cfo1* flower (J). K to M, Epidermal cells of lodicule in a *dl-sup1* flower (K), elongated lodicule (L), and efo in a *dl-sup1+cfo1* flower (M). The cells in K are part of the lodicule illustrated in I highlighted in the red box. The cells in L and M are parts of the lodicule in J highlighted in the red and yellow boxes, respectively. N, Relative expression levels of floral organ identity genes in *cfo1* and *cfo1+dl-sup1* floral organs. Error bars indicate SD. elo, Elongated lodicule; le, lemma; lo, lodicule; pa, palea; wt, wild type. Bars = 1,000 μm in A to D, G, H, and J, 500 μm in E, F, and I, 200 μm in K, and 100 μm in L and M. [See online article for color version of this figure.]

occurs in *osmads6* mutant flowers. In contrast, the *cfo1* mrp contained no vascular bundle, despite its lemma-like cellular structure. In addition, in *cfo1* flowers, ectopic *DL* expression was detected in the peripheral domains of lateral vascular bundles of the palea, whereas normal *DL* expression was detected in the peripheral domains of medial vascular bundles in the wild-type lemma. These findings indicate that the palea is not equivalent to the lemma in *cfo1* flowers. In addition, they imply that the *cfo1* mrp defects arise because cells in the peripheral domains of lateral vascular bundles follow a similar cellular developmental program to cells in the peripheral domains of medial vascular bundles in the lemma.

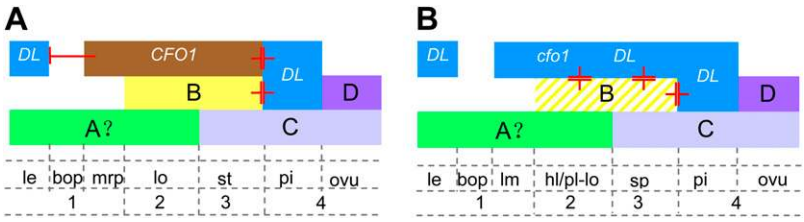

Figure 11. Roles of *CFO1* in the specification of rice floral organ identity. A, In wild-type rice flowers, B-, C-, and D-class genes, *CFO1* MADS box genes, and the *DL* gene determine floral organ identities. Although *DL* is mainly responsible for the specification of pistil identity, it also regulates lemma development. The *CFO1* and B-class genes repress *DL* expression in whorls 2 and 3, whereas *CFO1* also acts as a repressor of *DL* expression in the mrp. B, In *cfo1* flowers, *DL* is expressed ectopically in the mrp, which results in mrp identity conversion resembling the lemma, and the ectopic expression of *DL* leads to chimeric organs in whorls 2 and 3. hl/pl-lo, Hull- or pistil-like lodicule; le, lemma; lm, lemma-like mrp; lo, lodicule; ovu, ovule; sp, stamen-pistil chimera; st, stamen.

Role of *CFO1* in Lodicule Development

Lodicules are grass-specific organs that are considered to be homologous to dicot petals (Bommert et al., 2005; Whipple et al., 2007). The rice B-class genes *OsMADS2*, *OsMADS4*, and *OsMADS16* determine lodicule identity (Nagasawa et al., 2003; Prasad and Vijayraghavan, 2003; Xiao et al., 2003; Yadav et al., 2007; Yao et al., 2008). In plants that have nonfunctional copies of these genes, the lodicules are elongated or transformed into mrp-like structures. The *OsMADS6* gene also determines lodicule identity. Some *osmads6* flowers displayed hull-like lodicules, in which *OsMADS1*, *OsMADS14*, and *OsMADS15* were expressed ectopically at the heading stage (Ohmori et al., 2009; Li et al., 2010).

Our results here show that the lodicules are transformed into hull-lodicule or pistil-lodicule chimeras in the majority of *cfo1* flowers. In addition, the expression of B-class genes and *OsMADS6* was absent in partial domains of *cfo1* lodicules, whereas *OsMADS1*, *OsMADS13*, and *DL* were expressed ectopically in similar domains at an early stage of flower development. Given the phenotype of hull-lodicule or pistil-lodicule chimeras, the domains are possibly hull-like or pistil-like tissues. Thus, *CFO1* was shown to maintain proper lodicule identity by prevention of the establishment of hull- and pistil-like identities in lodicules, whereas *OsMADS6* prevented hull-like tissue formation, and B-class genes prevented mrp-like tissue formation, in whorl 2.

Hull-like lodicules developed in both the *osmads6* and *cfo1* mutants, which suggested that *OSMADS6* and *CFO1* contribute to prevent the establishment of hull-like identities in lodicules. However, the *osmads6* lodicule displayed complete hull-like histological identity in all of the cell layers (Ohmori et al., 2009). In contrast, the *cfo1* lodicule showed hull-like identity only in the silicified upper epidermis and not in the other tissues, of which the inner cell layers often displayed pistil-like identity. Therefore, *CFO1* and *OsMADS6* may function in different regulatory pathways to control lodicule identity.

CFO1 Regulates Asymmetrical Development in Whorl 2

In this investigation, efo were often observed on the palea side in whorl 2 of most *cfo1* flowers. In the same position, ectopic hull-like organs are observed in plants with loss of *OsMADS6* gene function (Yamaguchi et al., 2006). Ectopic lodicules develop in plants with loss of *OsMADS3* and *OsMADS58* gene function (Yamaguchi et al., 2006; Ohmori et al., 2009; Li et al., 2010). In wild-type rice flowers, two lodicules are located interior to the lemma instead of the palea, which is indicative of asymmetrical lodicule development in rice. Although the identities of the ectopic organs differ among these mutants, the formation of these organs strongly implies that the four MADS-box genes play an important role in the repression of ectopic organ initiation in whorl 2 and maintenance of the asymmetrical development of lodicules.

Rice flowers might have evolved from an ancestral species with flowers that possessed three lodicules (Clifford, 1987; Grass Phylogeny Working Group, 2001; Yamaguchi et al., 2006). Grasses comprise the basal grasses and BEP and PACMAD clades (Grass Phylogeny Working Group II, 2012). Flowers with three lodicules occur among the basal grasses and many species of Bambusoideae, a subfamily in the BEP clade, whereas other species in the BEP and PACMAD clades develop flowers with two lodicules. Therefore, it is hypothesized that flowers with two lodicules evolved near the base of the BEP+PACMAD clade. It is possible that *CFO1*-like, *OsMADS6*-like, *OsMADS3*-like, and *OsMADS58*-like genes evolved new functions involved in the regulation of the asymmetrical development of lodicules near the base of the BEP+PACMAD clade, with a subsequent reversal in Bambusoideae species. However, it remains unclear whether the four MADS box genes function in the same regulatory pathway. In addition, it would be interesting to determine the correlation between the asymmetrical arrangement of lodicules and the functions of related genes such as *CFO1*-like, *AGL6*-like, and C-class genes in additional grass species.

CFO1 Negatively Regulates *DL*

The *DL* gene, which is expressed in whorl 4 and specifies pistil identity, antagonizes *OsMADS16* gene function between whorls 3 and 4 (Nagasawa et al., 2003; Yamaguchi et al., 2004). In *spw1* mutants, ectopic expression of *DL* causes complete transformation of stamens into pistils in whorl 3 (Nagasawa et al., 2003; Yamaguchi et al., 2004). Whorls 2 and 3 of *cfo1* flowers contained various chimeras with fused pistil-like tissue and ectopic *DL* expression. These results imply that ectopic *DL* expression results in ectopic formation of pistil-like tissue.

The *DL* gene is also expressed in the peripheral domain of the medial vascular bundle of the lemma, but it is not clear whether *DL* controls lemma development (Fig. 6J; Yamaguchi et al., 2004). Recently, a defective lemma was reported in *dl-sup6*, an allelic mutant of *DL* (Li et al., 2011b). The *dl-sup6* lemmas displayed alternate numbers of vascular tissues (either three or four vascular bundles), whereas the wild-type lemma contains a characteristic five vascular bundles (Li et al., 2011b). This result suggested that *DL* has a function in the specification of lemma vascular bundles and their peripheral tissues. In our study, abundant *DL* transcripts were detected in the peripheral domain of lateral vascular bundles of the *cfo1* palea. On the basis of these results, it is reasonable to speculate that the ectopic *DL* activation in peripheral domains of lateral vascular bundles of the *cfo1* palea resulted in the domains undergoing a similar development pattern with the domains in the lemma, thereby causing transformation of the mrp into a lemma-like tissue. Similarly, the formation of hull-like tissues in the lodicule and efo of the *cfo1* flowers is probably caused by ectopic *DL* activation.

The mrp in the flower of the *cfo1+dl-sup1* double mutant has a normal phenotype, with no ectopic hull- or pistil-like tissues observed in whorls 2 and 3. This further confirms that ectopic *DL* activation causes the defects observed in the mrp, lodicule, and stamen of the *cfo1* flower. Thus, it is possible that *CFO1* plays a pivotal role in the maintenance of floral organ identity through repression of *DL* transcription in the mrp, lodicule, and stamen (Fig. 11A). When *CFO1* is dysfunctional, *DL* expression is extended, which results in a lemma-like mrp and chimeric organs in whorls 2 and 3 (Fig. 11B). We also observed that overexpression of *CFO1* did not result in *dl* phenotypes in the leaf, lemma, and pistil. Moreover, *CFO1* is expressed not only in the mrp in whorls 2 and 3 but also in the lemma and pistil. These results suggest that *CFO1* restriction of *DL* expression should depend on interaction with other factors in the mrp in whorls 2 and 3. Therefore, characterization of these factors will improve our understanding of the regulation of floral organ identity in rice.

CFO1 Is Also Required for Floral Meristem Development

In flowering plants, it is generally reported that many C- and E-class MADS box genes regulate the determination of the floral meristem in addition to floral organ identity. In general, mutation of these genes results in repeated organ occurrence in whorl 4 in severe cases or occasionally an increase in organ number (Mizukami and Ma, 1997; Jeon et al., 2000; Ditta et al., 2004; Ferrario et al., 2006; Yamaguchi et al., 2006; Ohmori et al., 2009; Li et al., 2010). In rice, loss of function of the C-class gene *OsMADS58* causes a complete loss of floral meristem determinacy, resulting in the indeterminate development of flowers that consist of lodicules, stamens, and a carpel-like organ in whorl 4. These results suggest that *OsMADS58* is crucial for the regulation of floral meristem determinacy in rice (Yamaguchi et al., 2006). Another C-class gene, *OsMADS3*, contributes weakly to this function, because multiple carpels developed in whorl 4 of *osmads3* flowers. The AGL6-like gene *OsMADS6* might be another major regulator of floral meristem determinacy. The *osmads6* mutant displayed repetitive formation of abnormal carpels and occasional immature spikelets in whorl 4, which suggests that floral meristem determinacy was affected seriously (Ohmori et al., 2009; Li et al., 2010). The SEP-like gene *LHS1/OsMADS1* also contributes weakly to the regulation of floral meristem determinacy. The *lhs1* mutant showed additional carpels and florets occasionally (Jeon et al., 2000).

In *cfo1* flowers, the initiation and development of floral organ primordia in whorls 3 and 4 were delayed, and the numbers of stamens and pistils were altered, which indicated that normal floral meristem development was disturbed. However, compared with the above-mentioned mutants, floral meristem determinacy was affected less by mutation of *CFO1*, because no repeated organs developed and the floral meristem was consumed by the pistils in *cfo1* flowers. These results suggest that *CFO1* is required for normal floral meristem development but contributes very weakly to the regulation of floral meristem determinacy.

CONCLUSION

In this study, we characterized the function of an ancient MIKC gene, *CFO1/OsMADS32*, in the regulation of floral organ identity in rice. The *cfo1* mutant displayed a lemma-like mrp, chimeric floral organs, and efo. Almost all of the known floral organ identity genes showed defective expression in *cfo1* flowers during the early and heading stages of flower development. In particular, we showed that the floral organ identity gene *DL* was expressed ectopically in all defective organs of *cfo1* flowers. Double mutant analysis revealed that loss of *DL* function mitigated most of the defects in floral organs of *cfo1* flowers. These results suggested that *CFO1* plays a pivotal role in the maintenance of floral organ identity through the repression of *DL* transcription in the mrp, lodicule, and stamens. Our findings extend the current understanding of the origin and diversification of the MADS box genes that contribute to the development of grass-specific floral organs.

MATERIALS AND METHODS

Plant Materials

Rice (*Oryza sativa*) *cfo1* is a spontaneous mutant obtained from the *indica* line 2B. Four F1 populations were produced by crossing the *cfo1* mutant with four *indica* rice cultivars: Luhui17, R2727, Ce64, and Luhui602. The crosses were performed in Chongqing, China, during the summer of 2004. The F1 populations were raised in Hainan, China, during the autumn of 2004. F2 populations were planted in Chongqing, China, during the summer of 2005.

Map-Based Cloning of *CFO1*

Approximately 5,000 F2 plants were obtained from crosses between *cfo1* and Luhui602, and 1,206 homozygotic mutants were selected for high-resolution mapping. Gene mapping was conducted using genetic markers obtained from publicly available rice databases, including Gramene (http://www.gramene.org) and RGP (http://rgp.dna.affrc.go.jp/publicdata/caps/index.html). Analysis of candidate genes was performed using a CAPS marker, sequencing, and complement testing. The sequences of primers used in the mapping and candidate gene analysis are listed in Supplemental Table S3.

Microscopy Analysis

Panicles were collected at different developmental stages and fixed in 50% ethanol, 0.9 M glacial acetic acid, and 3.7% formaldehyde overnight at 4°C, dehydrated with a graded ethanol series, infiltrated with xylene, and embedded in paraffin (Sigma). The 8-μm-thick sections were transferred onto poly-L-Lys-coated glass slides, deparaffinized in xylene, and dehydrated through an ethanol series. The sections were stained sequentially with 1% safranine (Amresco) and 1% Fast Green (Amresco), then dehydrated through an ethanol series, infiltrated with xylene, and finally mounted beneath a coverslip. Light microscopy was performed using a Nikon E600 microscope. For scanning electron microscopy, fresh samples were examined using a Hitachi S-3400 scanning electron microscope with a cool stage.

RT-PCR and qRT-PCR Analysis

Total RNA was isolated from various tissue samples using the RNeasy Plant Mini Kit (Waston). The first strand of cDNA was synthesized from 2 μg of total RNA using oligo$(dT)_{18}$ primers in a 25-μL reaction volume using the SuperScript III Reverse Transcriptase Kit (Invitrogen). One-half microliter of the reverse-transcribed RNA was used as a PCR template with gene-specific primers (Supplemental Table S3). *ACTIN* was used as an endogenous control. For RT-PCR, the PCR products were separated in 2% agarose containing 1× Tris-acetate-EDTA buffer. The qRT-PCR analysis was performed with an ABI Prism 7000 Sequence Detection System and the SYBR Supermix Kit (Bio-Rad). At least three replicates were performed to produce the mean values of each expression level.

Vector Construction

To construct the *OsMADS32* overexpression plasmids, the *OsMADS32* cDNA that contained the whole open reading frame and partial untranslated region was amplified using the primers M32OE-F and M32OE-R. The cDNA were inserted into the expression cassette pCA-35S-NOS. The constructs were transferred into calli of *japonica* rice 'Zhonghua11' by *Agrobacterium tumefaciens*-mediated T-DNA transformation as described previously (Xiao et al., 2009). The primer sequences are listed in Supplemental Table S3.

In Situ Hybridization

The 419-bp gene-specific *CFO1* probe was amplified with the primers M32H-F and M32H-R and labeled using the DIG RNA Labeling Kit (SP6/T7; Roche) in accordance with the vendor's recommendations. Probes for the known floral organ genes were prepared using the same method. Pretreatment of sections, hybridization, and immunological detection were performed as described previously (Xiao et al., 2009). The primer sequences are listed in Supplemental Table S3.

Phylogenetic Analysis

A phylogenetic tree derived from 153 MIKC protein sequences was constructed using MEGA version 5 (Tamura et al., 2011). One class that consisted of 12 MIKC*-type genes was regarded as the outgroup. The tree was constructed using the maximum likelihood method based on the Jones-Taylor-Thornton matrix-based model with the lowest Bayesian Information Criterion scores (Jones et al., 1992; Tamura et al., 2011). Bootstrap support values for each node from 500 replicates are shown next to the branches (Felsenstein, 1985). Initial trees for the heuristic search were obtained automatically as follows. When the number of common sites was less than 100 or less than one-fourth of the total number of sites, the maximum parsimony method was used; otherwise, the Bio-neighbor-joining method with Markov Cluster distance matrix was used. A discrete γ-distribution was used to model evolutionary rate differences among sites (five categories [+G]; parameter = 1.9631). The rate variation model allowed for some sites to be evolutionarily invariable ([+I]; 5.8060% sites). The tree is drawn to scale, with branch lengths measured in the number of substitutions per site. The analysis involved 153 amino acid sequences. All positions containing gaps and missing data were eliminated. There were a total of 109 positions in the final data set.

The GenBank accession numbers for the cDNA sequences of *CFO1*, *DL*, *OsMADS1*, *OsMADS2*, *OsMADS3*, *OsMADS4*, *OsMADS6*, *OsMADS13*, *OsMADS14*, *OsMADS15*, *OsMADS16*, and *OsMADS58* are HQ711850, AB106553, NM_001055911, AK070894, L37528, NM_001062125, FJ666318, NM_001072917, NM_001057835, NM_001065255, NM_001065095, and NM_001061424, respectively.

Supplemental Data

The following materials are available in the online version of this article.

Supplemental Figure S1. Statistical analysis of *cfo1* flowers.

Supplemental Figure S2. qRT-PCR analysis of floral organ identity gene expression in the inner floral organs of wild-type and *cfo1* flowers.

Supplemental Figure S3. Results of a CAPS assay of 32 recombinants from 1,206 F2 individuals.

Supplemental Figure S4. Analysis of *OsMADS32* overexpression plants.

Supplemental Figure S5. Molecular characterization of T-DNA insertion line AF36 and verification of allelism with *cfo1*.

Supplemental Figure S6. Protein sequence alignment of $MIKC^C$ genes in grasses.

Supplemental Figure S7. Scanning electron microscopy analysis of *dl-sup1* and *dl-sup1+cfo1* flowers at early stages.

Supplemental Table S1. Segregation of the *cfo1* allele in four F2 populations.

Supplemental Table S2. Segregation of F1 progeny with the M32OEm32oeCFO1cfo1 genotype in F2 populations.

Supplemental Table S3. Primers used in the study.

ACKNOWLEDGMENTS

We gratefully acknowledge Dr. Changyin Wu from the National Center of Plant Gene Research (Wuhan, China) for providing the *OsMADS32* T-DNA insertion lines as well as Dr. Yasuo Nagato of the University of Tokyo and Prof. Lihuang Zhu from the Institute of Genetics and Developmental Biology (Beijing, China) for providing the *dl-sup1* mutants. We also thank Prof. Yan Pei from Southwest University (Chongqing, China) for providing the rice transformation vectors.

Received May 23, 2012; accepted August 10, 2010; published August 13, 2012.

LITERATURE CITED

Agrawal GK, Abe K, Yamazaki M, Miyao A, Hirochika H (2005) Conservation of the E-function for floral organ identity in rice revealed by the analysis of tissue culture-induced loss-of-function mutants of the *OsMADS1* gene. Plant Mol Biol **59:** 125–135

Alvarez-Buylla ER, Pelaz S, Liljegren SJ, Gold SE, Burgeff C, Ditta GS, Ribas de Pouplana L, Martínez-Castilla L, Yanofsky MF (2000) An

ancestral MADS-box gene duplication occurred before the divergence of plants and animals. Proc Natl Acad Sci USA **97:** 5328–5333

Arora R, Agarwal P, Ray S, Singh AK, Singh VP, Tyagi AK, Kapoor S (2007) MADS-box gene family in rice: genome-wide identification, organization and expression profiling during reproductive development and stress. BMC Genomics **8:** 242

Bommert P, Satoh-Nagasawa N, Jackson D, Hirano HY (2005) Genetics and evolution of inflorescence and flower development in grasses. Plant Cell Physiol **46:** 69–78

Bowman JL, Drews GN, Meyerowitz EM (1991) Expression of the *Arabidopsis* floral homeotic gene *AGAMOUS* is restricted to specific cell types late in flower development. Plant Cell **3:** 749–758

Bowman JL, Smyth DR (1999) *CRABS CLAW*, a gene that regulates carpel and nectary development in Arabidopsis, encodes a novel protein with zinc finger and helix-loop-helix domains. Development **126:** 2387–2396

Bowman JL, Smyth DR, Meyerowitz EM (1989) Genes directing flower development in *Arabidopsis*. Plant Cell **1:** 37–52

Chen ZX, Wu JG, Ding WN, Chen HM, Wu P, Shi CH (2006) Morphogenesis and molecular basis on naked seed rice, a novel homeotic mutation of *OsMADS1* regulating transcript level of AP3 homologue in rice. Planta **223:** 882–890

Clifford HT (1987) Spikelet and floral morphology. *In* TR Soderstrom, KW Hilu, CS Campbell, ME Barkworth, eds, Grass Systematics and Evolution. Smithsonian Institution Press, Washington, DC, pp 21–30

Coen ES, Meyerowitz EM (1991) The war of the whorls: genetic interactions controlling flower development. Nature **353:** 31–37

Ditta G, Pinyopich A, Robles P, Pelaz S, Yanofsky MF (2004) The *SEP4* gene of *Arabidopsis thaliana* functions in floral organ and meristem identity. Curr Biol **14:** 1935–1940

Dreni L, Jacchia S, Fornara F, Fornari M, Ouwerkerk PB, An G, Colombo L, Kater MM (2007) The D-lineage MADS-box gene *OsMADS13* controls ovule identity in rice. Plant J **52:** 690–699

Drews GN, Bowman JL, Meyerowitz EM (1991) Negative regulation of the Arabidopsis homeotic gene *AGAMOUS* by the *APETALA2* product. Cell **65:** 991–1002

Felsenstein J (1985) Confidence limits on phylogenies: an approach using the bootstrap. Evolution **39:** 783–791

Ferrario S, Shchennikova AV, Franken J, Immink RGH, Angenent GC (2006) Control of floral meristem determinacy in petunia by MADS-box transcription factors. Plant Physiol **140:** 890–898

Fornara F, Marziani G, Mizzi L, Kater M, Colombo L (2003) MADS-box genes controlling flower development in rice. Plant Biol **5:** 16–22

Goto K, Meyerowitz EM (1994) Function and regulation of the Arabidopsis floral homeotic gene *PISTILLATA*. Genes Dev **8:** 1548–1560

Grass Phylogeny Working Group (2001) Phylogeny and subfamilial classification of the grasses (Poaceae). Ann Mo Bot Gard **88:** 373–457

Grass Phylogeny Working Group II (2012) New grass phylogeny resolves deep evolutionary relationships and discovers C4 origins. New Phytol **193:** 304–312

Ikeda K, Sunohara H, Nagato Y (2004) Developmental course of inflorescence and spikelet in rice. Breed Sci **54:** 147–156

Itoh J, Nonomura K, Ikeda K, Yamaki S, Inukai Y, Yamagishi H, Kitano H, Nagato Y (2005) Rice plant development: from zygote to spikelet. Plant Cell Physiol **46:** 23–47

Jack T, Fox GL, Meyerowitz EM (1994) Arabidopsis homeotic gene *APETALA3* ectopic expression: transcriptional and posttranscriptional regulation determine floral organ identity. Cell **76:** 703–716

Jeon JS, Jang S, Lee S, Nam J, Kim C, Lee SH, Chung YY, Kim SR, Lee YH, Cho YG, et al (2000) *leafy hull sterile1* is a homeotic mutation in a rice MADS box gene affecting rice flower development. Plant Cell **12:** 871–884

Jin Y, Luo Q, Tong HN, Wang AJ, Cheng ZJ, Tang JF, Li DY, Zhao XF, Li XB, Wan JM, et al (2011) An AT-hook gene is required for palea formation and floral organ number control in rice. Dev Biol **359:** 277–288

Jofuku KD, den Boer BGW, Van Montagu M, Okamuro JK (1994) Control of *Arabidopsis* flower and seed development by the homeotic gene *APETALA2*. Plant Cell **6:** 1211–1225

Jones DT, Taylor WR, Thornton JM (1992) The rapid generation of mutation data matrices from protein sequences. Comput Appl Biosci **8:** 275–282

Kater MM, Dreni L, Colombo L (2006) Functional conservation of MADS-box factors controlling floral organ identity in rice and Arabidopsis. J Exp Bot **57:** 3433–3444

Kellogg EA (2001) Evolutionary history of the grasses. Plant Physiol **125:** 1198–1205

Kobayashi K, Maekawa M, Miyao A, Hirochika H, Kyozuka J (2010) *PANICLE PHYTOMER2* (*PAP2*), encoding a SEPALLATA subfamily MADS-box protein, positively controls spikelet meristem identity in rice. Plant Cell Physiol **51:** 47–57

Li HF, Liang WQ, Hu Y, Zhu L, Yin CS, Xu J, Dreni L, Kater MM, Zhang DB (2011a) Rice *MADS6* interacts with the floral homeotic genes *SUPERWOMAN1*, *MADS3*, *MADS58*, *MADS13*, and *DROOPING LEAF* in specifying floral organ identities and meristem fate. Plant Cell **23:** 2536–2552

Li HF, Liang WQ, Jia RD, Yin CS, Zong J, Kong HZ, Zhang DB (2010) The AGL6-like gene *OsMADS6* regulates floral organ and meristem identities in rice. Cell Res **20:** 299–313

Li HF, Liang WQ, Yin CS, Zhu L, Zhang DB (2011b) Genetic interaction of OsMADS3, DROOPING LEAF, and OsMADS13 in specifying rice floral organ identities and meristem determinacy. Plant Physiol **156:** 263–274

Luo Q, Zhou KD, Zhao XF, Zeng QC, Xia HG, Zhai WX, Xu JC, Wu XJ, Yang HS, Zhu LH (2005) Identification and fine mapping of a mutant gene for *palealess spikelet* in rice. Planta **221:** 222–230

Ma H, Yanofsky MF, Meyerowitz EM (1991) *AGL1-AGL6*, an Arabidopsis gene family with similarity to floral homeotic and transcription factor genes. Genes Dev **5:** 484–495

Malcomber ST, Kellogg EA (2004) Heterogeneous expression patterns and separate roles of the *SEPALLATA* gene *LEAFY HULL STERILE1* in grasses. Plant Cell **16:** 1692–1706

Malcomber ST, Kellogg EA (2005) *SEPALLATA* gene diversification: brave new whorls. Trends Plant Sci **10:** 427–435

Malcomber ST, Preston JC, Reinheimer R, Kossuth J, Kellogg EA (2006) Developmental gene evolution and the origin of grass inflorescence diversity. Adv Bot Res **44:** 425–481

Mandel MA, Gustafson-Brown C, Savidge B, Yanofsky MF (1992) Molecular characterization of the Arabidopsis floral homeotic gene *APETALA1*. Nature **360:** 273–277

Mizukami Y, Ma H (1997) Determination of *Arabidopsis* floral meristem identity by *AGAMOUS*. Plant Cell **9:** 393–408

Nagasawa N, Miyoshi M, Sano Y, Satoh H, Hirano H, Sakai H, Nagato Y (2003) *SUPERWOMAN1* and *DROOPING LEAF* genes control floral organ identity in rice. Development **130:** 705–718

Nam J, Kim J, Lee S, An GH, Ma H, Nei MS (2004) Type I MADS-box genes have experienced faster birth-and-death evolution than type II MADS-box genes in angiosperms. Proc Natl Acad Sci USA **101:** 1910–1915

Ohmori S, Kimizu M, Sugita M, Miyao A, Hirochika H, Uchida E, Nagato Y, Yoshida H (2009) *MOSAIC FLORAL ORGANS1*, an *AGL6*-like MADS box gene, regulates floral organ identity and meristem fate in rice. Plant Cell **21:** 3008–3025

Pelaz S, Ditta GS, Baumann E, Wisman E, Yanofsky MF (2000) B and C floral organ identity functions require *SEPALLATA* MADS-box genes. Nature **405:** 200–203

Pinyopich A, Ditta GS, Savidge B, Liljegren SJ, Baumann E, Wisman E, Yanofsky MF (2003) Assessing the redundancy of MADS-box genes during carpel and ovule development. Nature **424:** 85–88

Prasad K, Parameswaran S, Vijayraghavan U (2005) *OsMADS1*, a rice MADS-box factor, controls differentiation of specific cell types in the lemma and palea and is an early-acting regulator of inner floral organs. Plant J **43:** 915–928

Prasad K, Vijayraghavan U (2003) Double-stranded RNA interference of a rice *PI/GLO* paralog, *OsMADS2*, uncovers its second-whorl-specific function in floral organ patterning. Genetics **165:** 2301–2305

Tamura K, Peterson D, Peterson N, Stecher G, Nei M, Kumar S (2011) MEGA5: molecular evolutionary genetics analysis using maximum likelihood, evolutionary distance, and maximum parsimony methods. Mol Biol Evol **28:** 2731–2739

Theissen G, Kim JT, Saedler H (1996) Classification and phylogeny of the MADS-box multigene family suggest defined roles of MADS-box gene subfamilies in the morphological evolution of eukaryotes. J Mol Evol **43:** 484–516

Theissen G, Saedler H (2001) Plant biology: floral quartets. Nature **409:** 469–471

Wang K, Tang D, Hong L, Xu W, Huang J, Li M, Gu M, Xue Y, Cheng Z (2010) *DEP* and *AFO* regulate reproductive habit in rice. PLoS Genet **6:** e1000818

Weigel D, Meyerowitz EM (1994) The ABCs of floral homeotic genes. Cell **78:** 203–209

Whipple CJ, Zanis MJ, Kellogg EA, Schmidt RJ (2007) Conservation of B class gene expression in the second whorl of a basal grass and outgroups links the origin of lodicules and petals. Proc Natl Acad Sci USA **104:** 1081–1086

Xiao H, Tang JF, Li YF, Wang WM, Li XB, Jin L, Xie R, Luo HF, Zhao XF, Meng Z, et al (2009) *STAMENLESS 1*, encoding a single C2H2 zinc finger protein, regulates floral organ identity in rice. Plant J **59:** 789–801

Xiao H, Wang Y, Liu DF, Wang WM, Li XB, Zhao XF, Xu JC, Zhai WX, Zhu LH (2003) Functional analysis of the rice *AP3* homologue *OsMADS16* by RNA interference. Plant Mol Biol **52:** 957–966

Yadav SR, Prasad K, Vijayraghavan U (2007) Divergent regulatory *OsMADS2* functions control size, shape and differentiation of the highly derived rice floret second-whorl organ. Genetics **176:** 283–294

Yamaguchi T, Lee DY, Miyao A, Hirochika H, An GH, Hirano HY (2006) Functional diversification of the two C-class MADS box genes *OSMADS3* and *OSMADS58* in *Oryza sativa*. Plant Cell **18:** 15–28

Yamaguchi T, Nagasawa N, Kawasaki S, Matsuoka M, Nagato Y, Hirano HY (2004) The *YABBY* gene DROOPING *LEAF* regulates carpel specification and midrib development in *Oryza sativa*. Plant Cell **16:** 500–509

Yao SG, Ohmori S, Kimizu M, Yoshida H (2008) Unequal genetic redundancy of rice *PISTILLATA* orthologs, *OsMADS2* and *OsMADS4*, in lodicule and stamen development. Plant Cell Physiol **49:** 853–857

Zhang J, Li C, Wu C, Xiong L, Chen G, Zhang Q, Wang S (2006) RMD: a rice mutant database for functional analysis of the rice genome. Nucleic Acids Res **34:** D745–D748